Recent measurements of diboson production (including VBS)

Elvira Rossi[1]
On behalf of ATLAS and CMS Collaborations

[1]Università Federico II and INFN Napoli

SM@LHC Workshop 2025
APRIL 7-10, Durham


Why Diboson or multibosons?

- Stringent test of the Standard Model of electroweak gauge interactions
- VV: abundant production with relatively clean final state signatures
- Measurements of cross-section and polarization to validate the standard model (SM) at TeV scale
- Triple/Quartic Gauge boson coupling (T/QGC) to search for anomalous couplings and probe new physics ➔ EFT interpretation
- Vector boson scattering/fusion (VBS/VBF) processes (with relative lower cross-section) to probe the mechanism of electroweak symmetry breaking

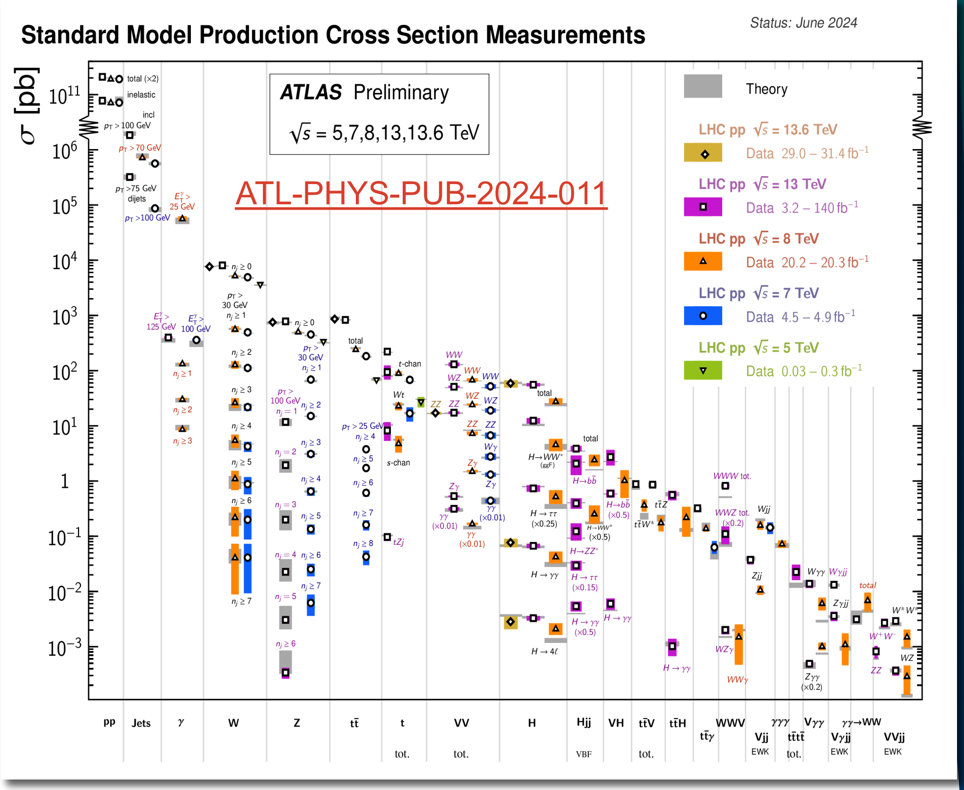

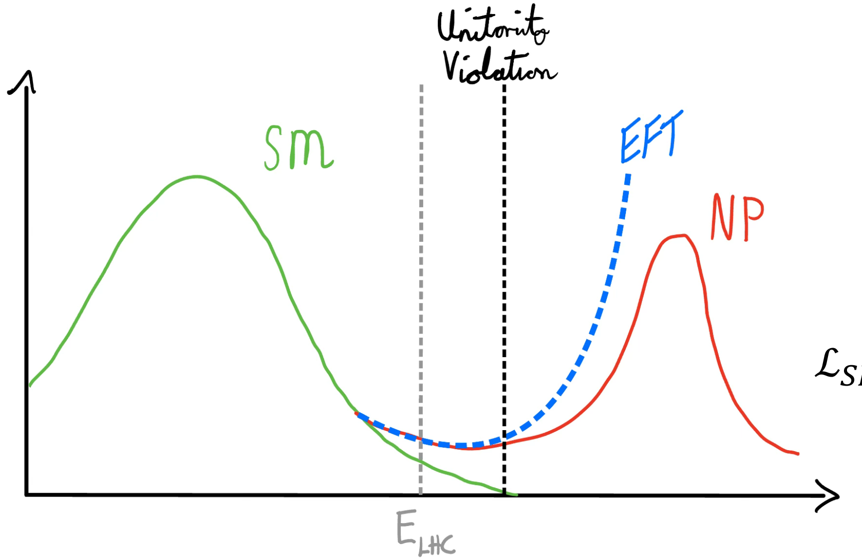

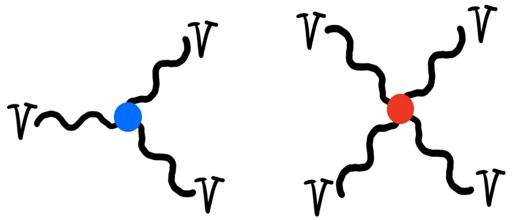

$$\mathcal{L}_{SMEFT} \approx \mathcal{L}_{SM}^{(4)} + \sum_i \frac{c_i^{(6)}}{\Lambda^2}\mathcal{O}_i^{(6)} + \sum_i \frac{c_i^{(8)}}{\Lambda^8}\mathcal{O}_i^{(8)}$$

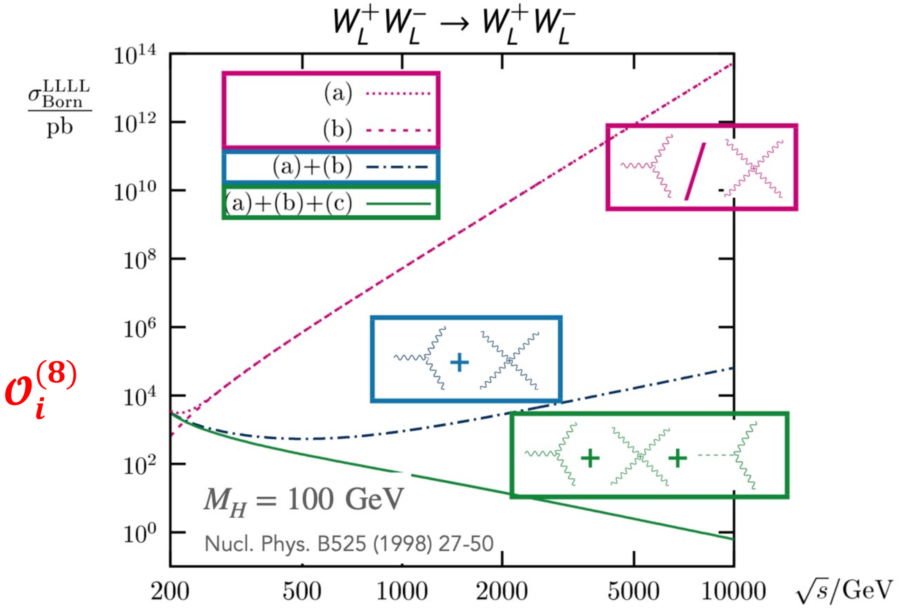

Outline and analyses overview

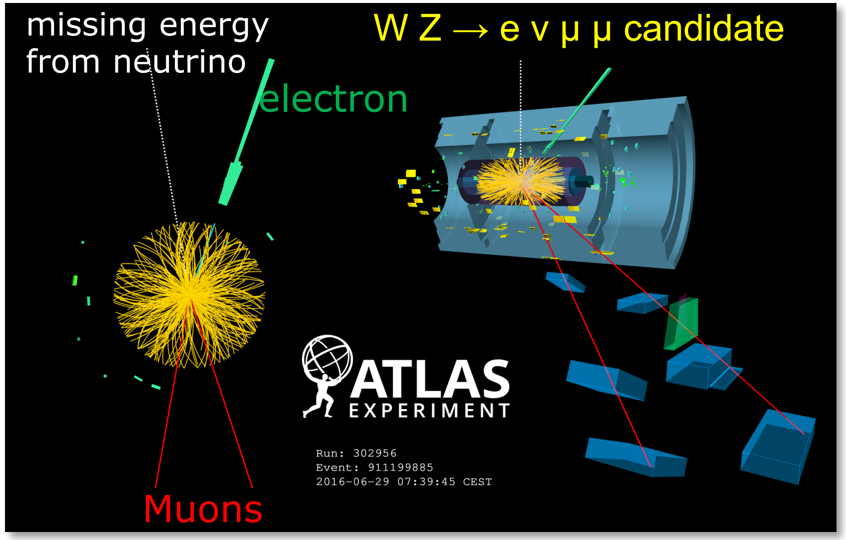

Inclusive WZ and differential cross section arXiv:2412.02477

Inclusive WW and differential cross section arXiv:2406.05101

Evidence for longitudinally polarised bosons in the EW $W^{\pm}W^{\pm}$ production arXiv:2503.11317

neutral Triple Gauge Couplings (nTGC) in $Z\gamma$ production ATLAS-COM-CONF-2025-005

VBS analyses:

EW diboson production in semileptonic final states at 13 TeV arXiv:2503.17461

Semileptonic VBS and anomalous quartic gauge couplings at 13 TeV CMS-PAS-SMP-22-011

Same-sign W boson scattering in events with one tau lepton arXiv:2410.04210

Fully- and semi-leptonic final states combination CMS-PAS-SMP-24-013

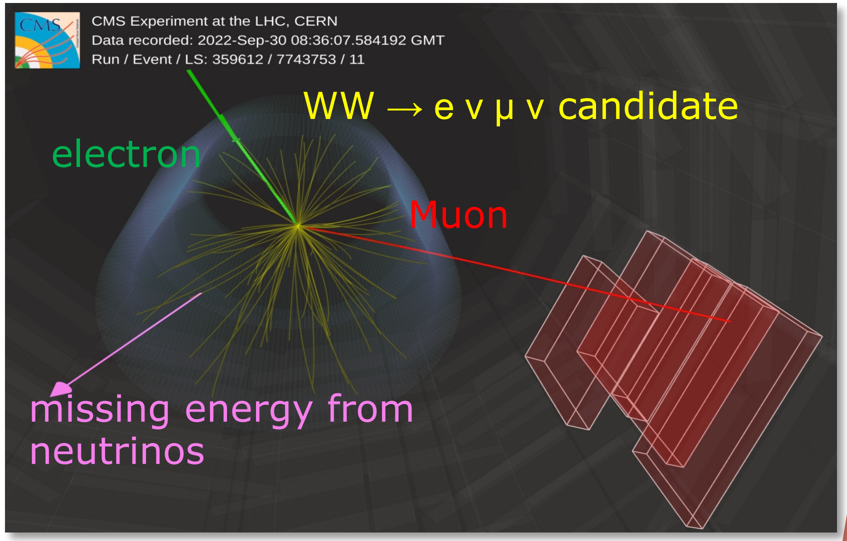

Updates recent measurements on Tribosons in Talk

EFT interpretation on experimental recent VBS Results Tobias's talk

Inclusive WZ production cross section

Submitted to J. High Energy Phys. - arXiv:2412.02477

- *WZ production @LHC is dominated by quark-antiquark annihilation at tree level ➔ the process is sensitive to TGCs that could modify the WZ production cross section and thus provide evidence of beyond-the-SM (BSM) physics.*
- *WZ is one of the main backgrounds for many SM measurements and BSM searches in multileptonic final states*
- *The measurement uses multileptonic final states and a simultaneous likelihood fit to the number of events in four different lepton flavour categories*

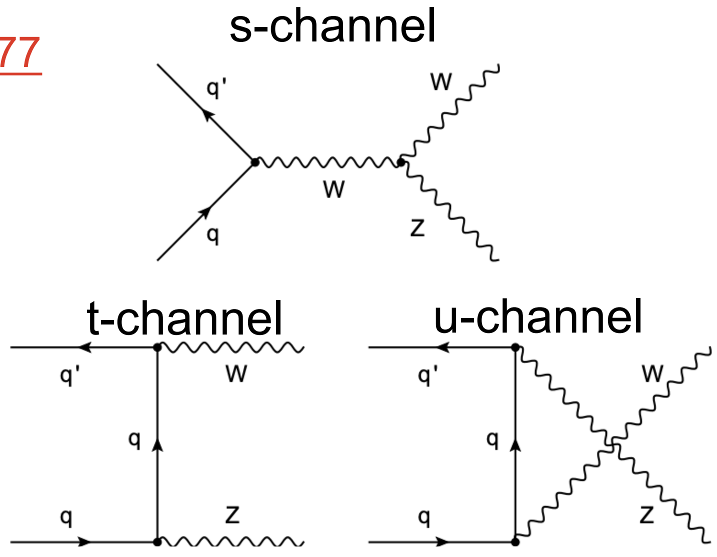

Multilepton final states with four lepton flavour categories: eee, eeμ, μμe, and μμμ

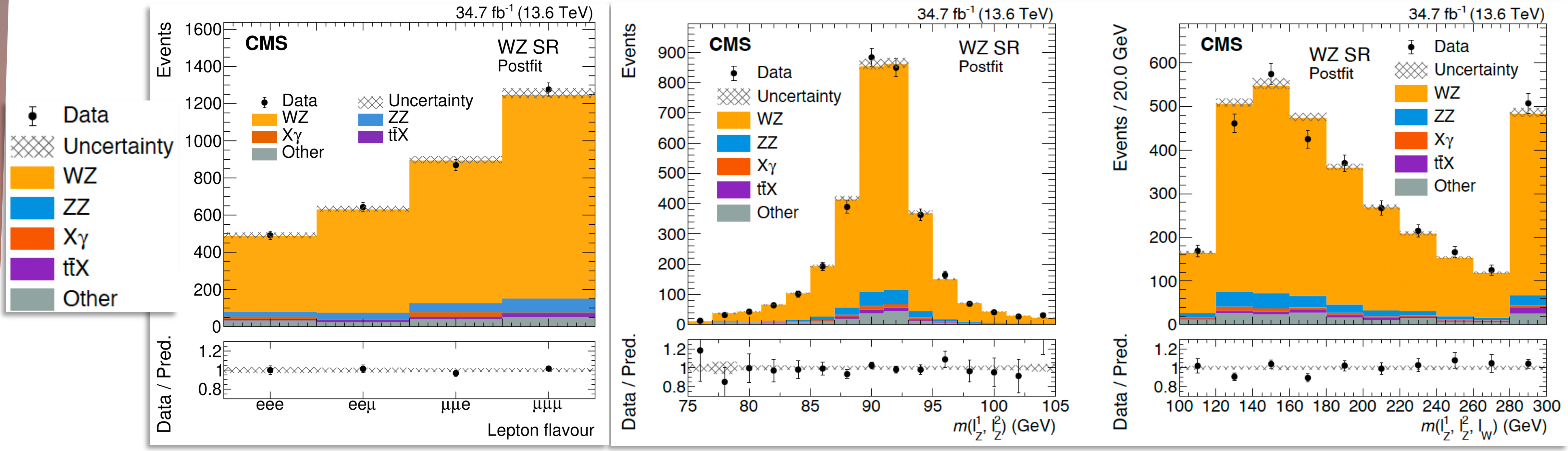

Inclusive WZ production cross section

Submitted to J. High Energy Phys. - arXiv:2412.02477

Total WZ production cross section

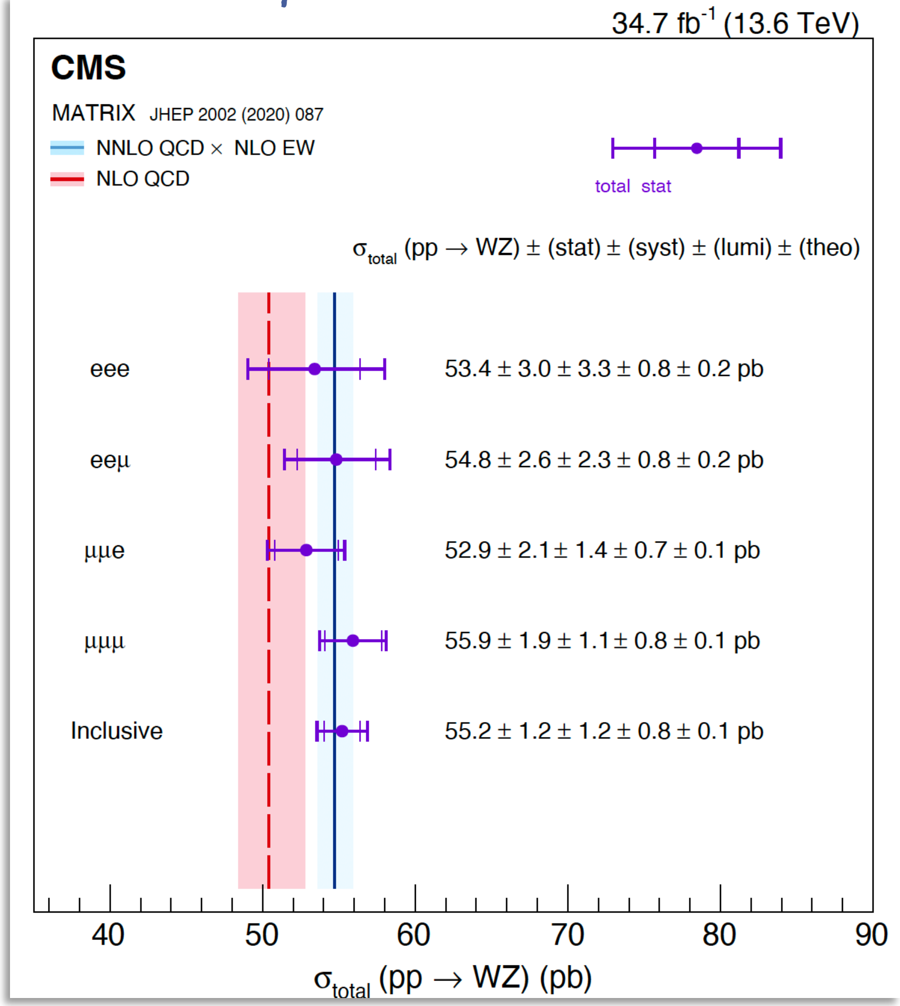

measurements in agreement with standard model predictions

Flavour-inclusive total cross section predictions

Accuracy	Total cross section (pb)
POWHEG, NLO QCD	$50.5\,^{+2.6}_{-2.1}$ (scale) $\pm\,1.1$ (PDF)
MATRIX, NLO QCD	$50.4\,^{+2.3}_{-2.0}$ (scale)
MATRIX, NNLO QCD	$55.0\,^{+1.2}_{-1.1}$ (scale)
MATRIX, NNLO QCD × NLO EW	$54.7\,^{+1.2}_{-1.1}$ (scale)

Inclusive (Measured) $55.2 \pm 1.2\,(\text{stat}) \pm 1.2\,(\text{syst}) \pm 0.8\,(\text{lumi}) \pm 0.1\,(\text{theo})$ pb

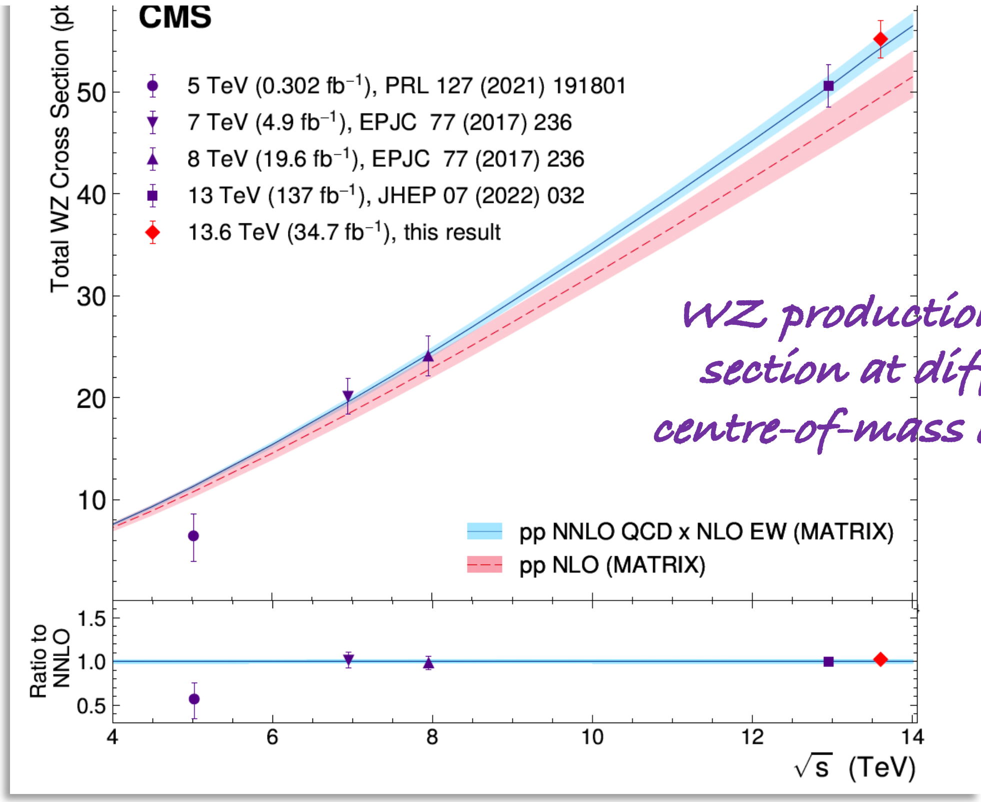

WZ production cross section at different centre-of-mass energies

Inclusive WW and differential cross section

Accepted by Phys. Lett. B. - arXiv:2406.05101

W^+W^- production cross section at $\sqrt{s}$ = 13.6 TeV

- Maximum likelihood fit in signal- and background-enriched categories (WW Signal Region (SR) and the one/two b tags, $Z \rightarrow \tau\tau$, same-sign, WZ and ZZ Control Regions (CR)) defined by the flavour and charge of the leptons, the number of jets, and number of b-jets.

W^+W^- production cross sections is an important test of the standard model:

- sensitive EW boson self-interactions properties and a test of the predictions of perturbative QCD and the EW theory
- large background in the measurement of Higgs boson production, in searches for BSM physics and in tt production studies
- It is important to model the production of WW+jets accurately in event generators.

$W^+W^- \longrightarrow e^{\pm}\nu\mu^{\mp}\nu$

number of reconstructed jets

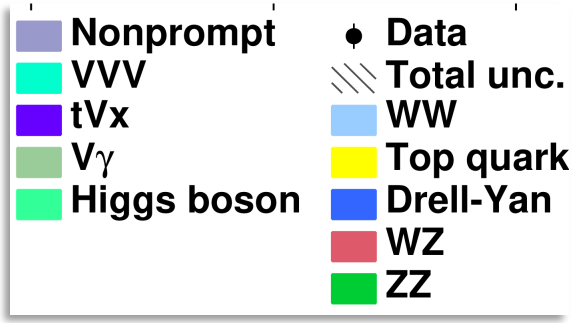

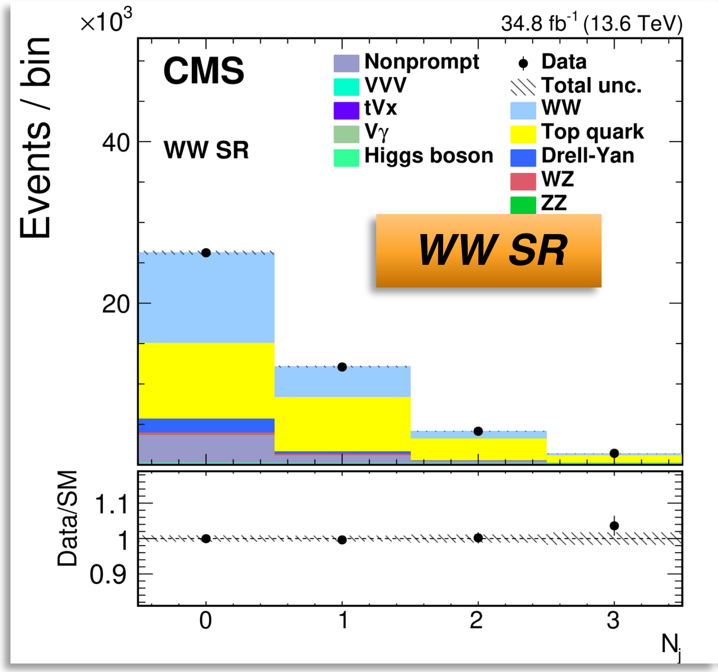

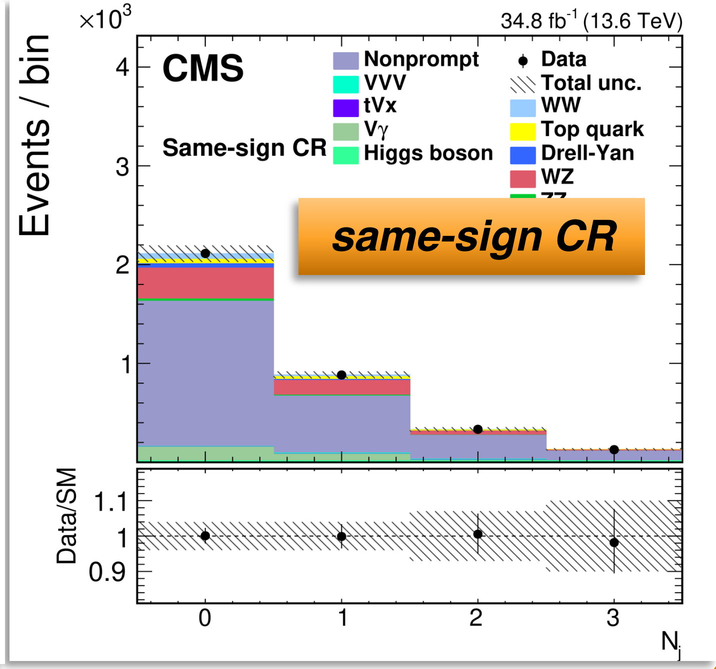

Inclusive WW and differential cross section

Accepted by Phys. Lett. B. - arXiv:2406.05101

Inclusive WW production cross section at √s = 13.6 TeV

$$\sigma = 125.7 \pm 2.3(stat) \pm 4.8(\mathrm{syst}) \pm 1.8(\mathrm{lumi}) = 125.5 \pm 5.6\ \mathrm{pb}$$

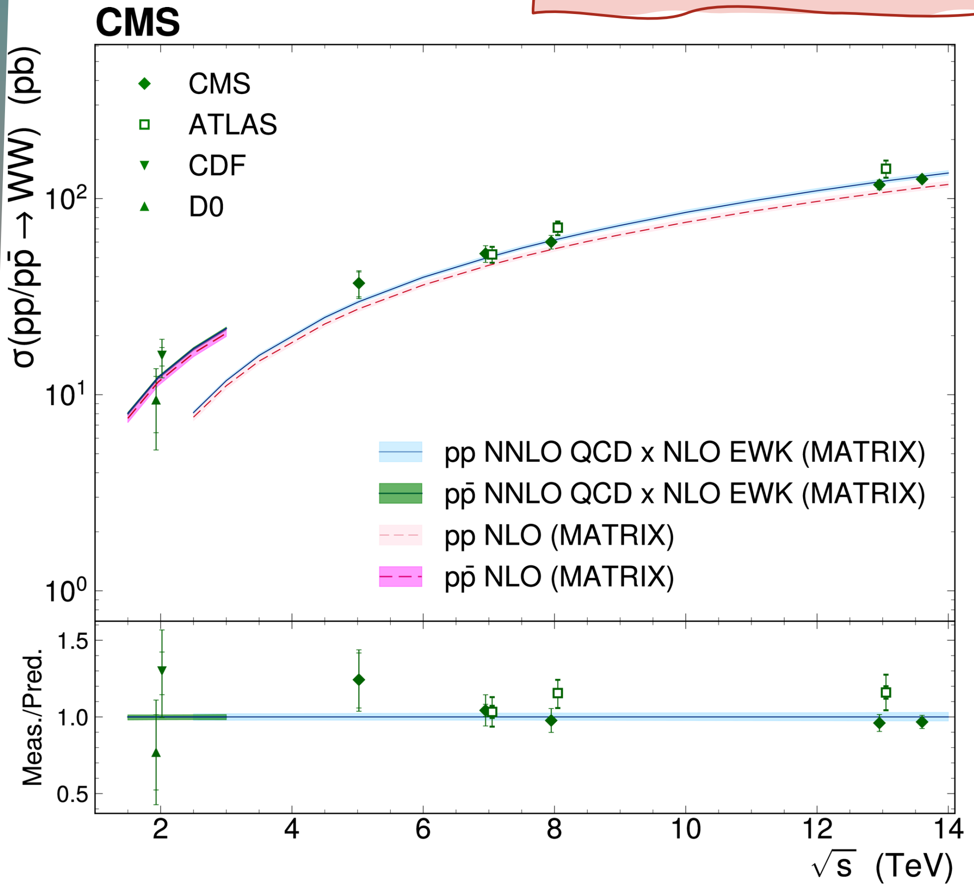

Uncertainties impact on signal strength (μ)

Uncertainty source	$\Delta\mu$
Integrated luminosity	0.014
Lepton experimental	0.019
Jet experimental	0.008
b tagging	0.012
Nonprompt background	0.010
Limited sample size	0.017
Background normalization	0.018
Theory	0.011
Statistical	0.018
Total	0.044

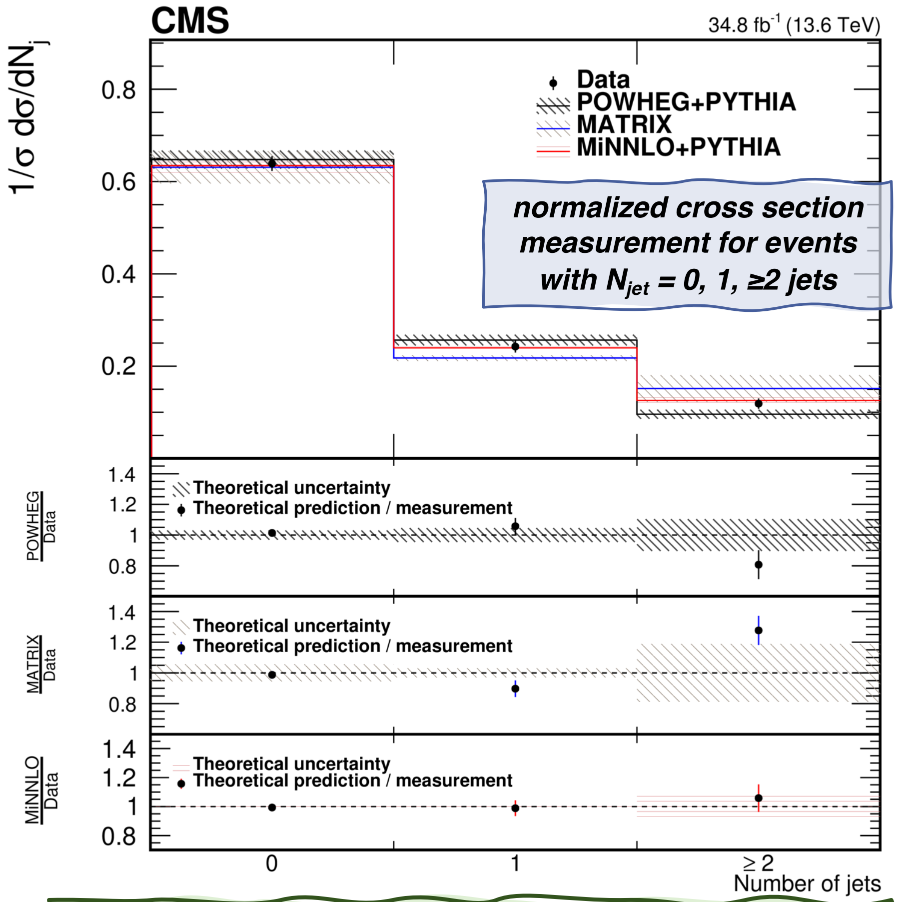

normalized cross section measurement for events with N_{jet} = 0, 1, ≥2 jets

The overall sensitivity is about 25% better than previous CMS measurements at √s = 13 TeV with a similar integrated luminosity, because of several reduced experimental uncertainties and the improved fit strategy

The measured fdifferential cross sections agree with the theoretical predictions within uncertainties.

Same-sign W boson polarisation

- Based on Run 2 cross-section measurement 2312.00420
- Updated with state-of-art Sherpa3 polarisation modelling with NLO EW & QCD corrections
- Frame dependant measurement using **Deep Neural Networks** built for:
  - **DNN$_{\text{inclusive}}$**: EW $W^{\pm}W^{\pm}jj$ – background discrimination
  - **LL - DNN$_{\text{signal}}$**: $W_L^{\pm}W_L^{\pm}$ – $W_T^{\pm}W_X^{\pm}$ (with X=L,T) discrimination
  - **LX - DNN$_{\text{signal}}$**: $W_L^{\pm}W_X^{\pm}$ – $W_T^{\pm}W_T^{\pm}$ discrimination
- DNNs trained with up to 20 input variables such as $\Delta\eta_{\ell\ell}$, $\boldsymbol{m_{\ell\ell}}$, $\boldsymbol{\Delta\phi_{jj}}$, m_{jj}, m_T^{o}, $m_T^{\ell_2}$, $p_T^{j_i}$, …

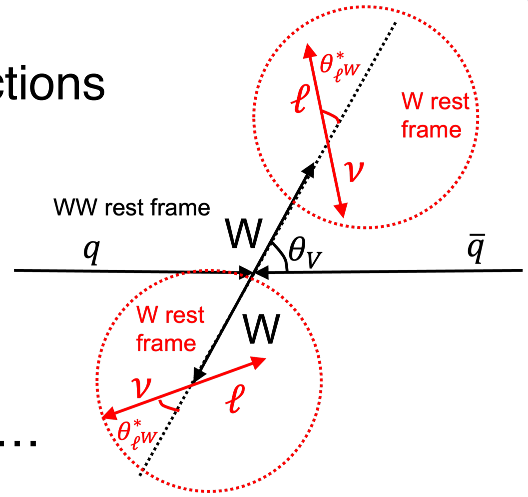

VBS EW $W^{\pm}W^{\pm}jj$ production

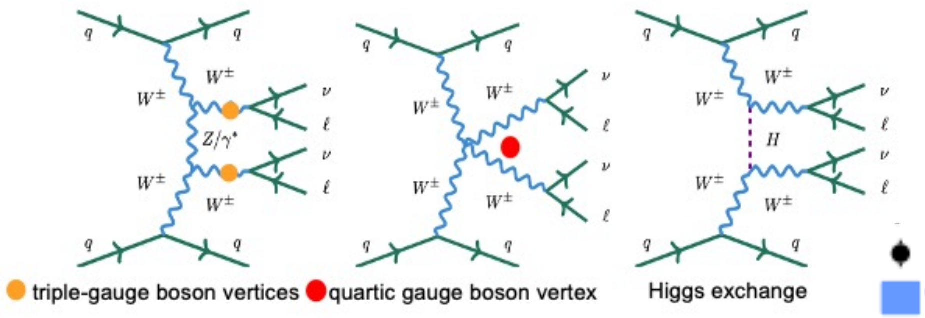

QCD $W^{\pm}W^{\pm}jj$ production

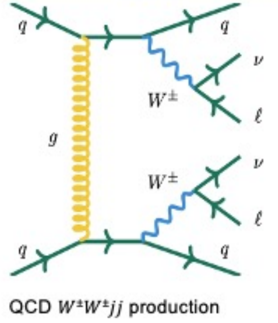

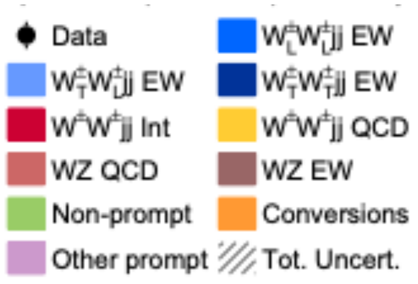

Higher-ranked variables in Signal Region

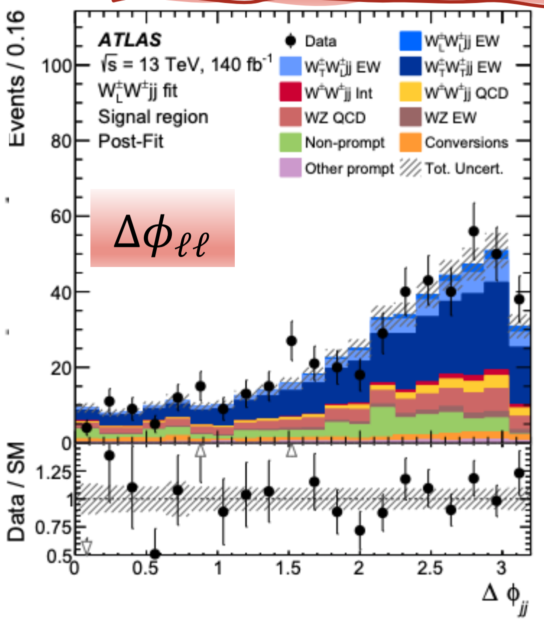

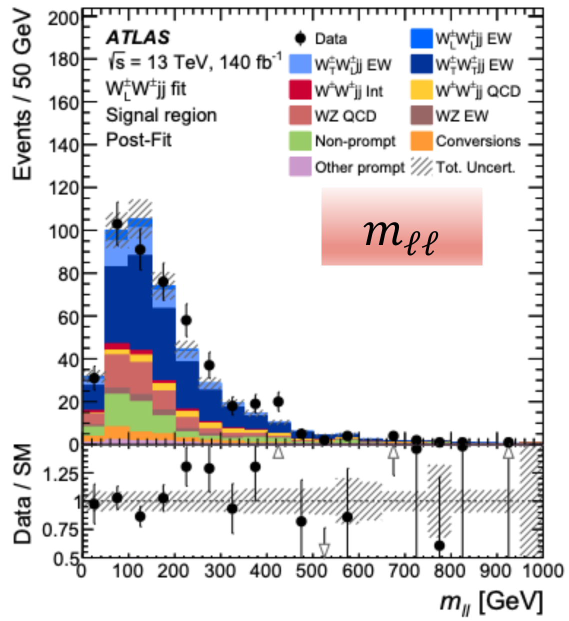

Same-sign W boson polarisation

- Two fits performed to extract the $W_L^{\pm}W_X^{\pm}$ and $W_T^{\pm}W_T^{\pm}$ ($W_L^{\pm}W_L^{\pm}$ and $W_T^{\pm}W_X^{\pm}$) polarisation fractions:
  - Fit performed in 3 regions of **DNN** **$\text{DNN}_{\text{inclusive}}$**: **$\text{LL-DNN}_{\text{signal}}$** as a polarisation discriminator and low-m_{jj} and WZ CRs also enter the fit
  - **No significant excess consistent with $W_L^{\pm}W_L^{\pm}$ is observed**

95% CL limits calculated on the fiducial cross-section times BR:

Observed $\sigma B(W_L^{\pm}W_L^{\pm}) = 0.45\ fb$

Expected $\sigma B(W_L^{\pm}W_L^{\pm}) = 0.70\ fb$

$\text{LL-DNN}_{\text{signal}}$: $W_L^{\pm}W_L^{\pm}$ – $W_T^{\pm}W_X^{\pm}$ discrimination

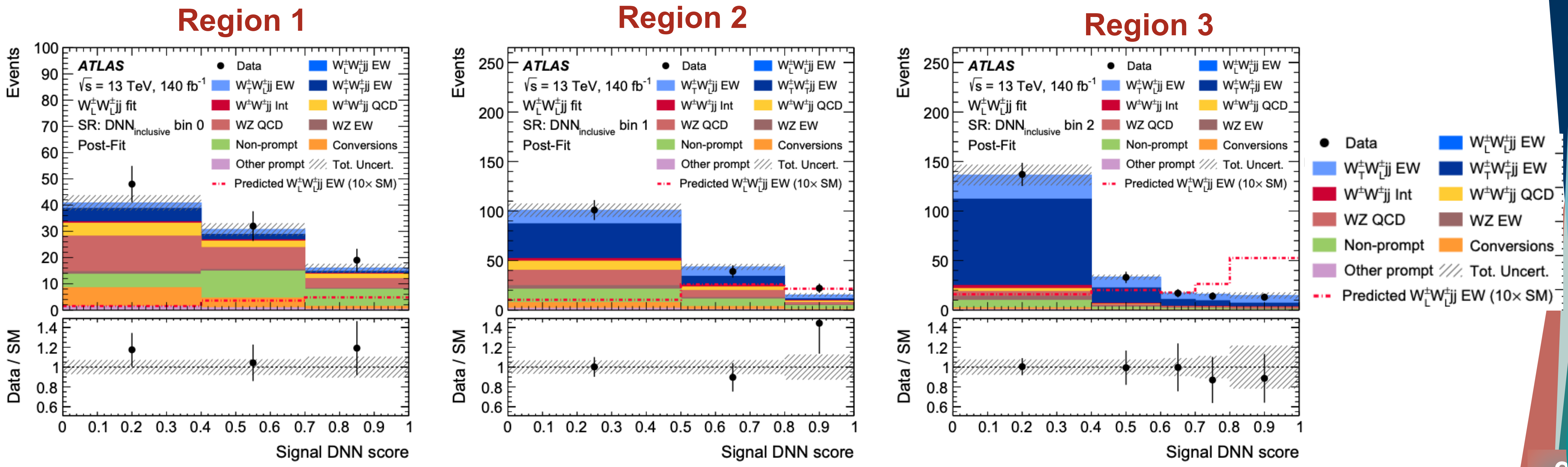

Same-sign W boson polarisation

- Two fits performed to extract the $W_L^{\pm}W_X^{\pm}$ and $W_T^{\pm}W_T^{\pm}$ ($W_L^{\pm}W_L^{\pm}$ and $W_T^{\pm}W_X^{\pm}$) polarisation fractions
  - Fit performed in 3 regions of $\text{DNN}_{\text{inclusive}}$: **$\text{LX-DNN}_{\text{signal}}$** as a polarisation discriminator and low- m_{jj} and WZ CRs also enter the fit
    - Evidence of $W_L^{\pm}W_X^{\pm}$ state: **3.3σ observed (4.0σ expected)**
    - Measurement precision is **statistically** limited

Source of uncertainty	Impact [%]
Experimental	
Lepton calibration	0.2
Jet energy and E_T^{miss} scale and resolution	3.9
Pileup modelling	1.2
Background, misid. leptons	4.2
Background, charge misrec.	0.5
Luminosity	1.1
Modeling	
$W^{\pm}W^{\pm}jj$ EW + QCD uncertainties	4.7
Background, WZ scale, PDFs & α_s	0.4
Background, WZ reweighting	0.3
Model statistical	7.2
Small background normalizations	1.1
Normalisation factors	2.5
Experimental and modelling	11.1
Data statistical	34.1
Total	34.1

$\text{LX-DNN}_{\text{signal}}$: $W_L^{\pm}W_X^{\pm}$ – $W_T^{\pm}W_T^{\pm}$ discrimination

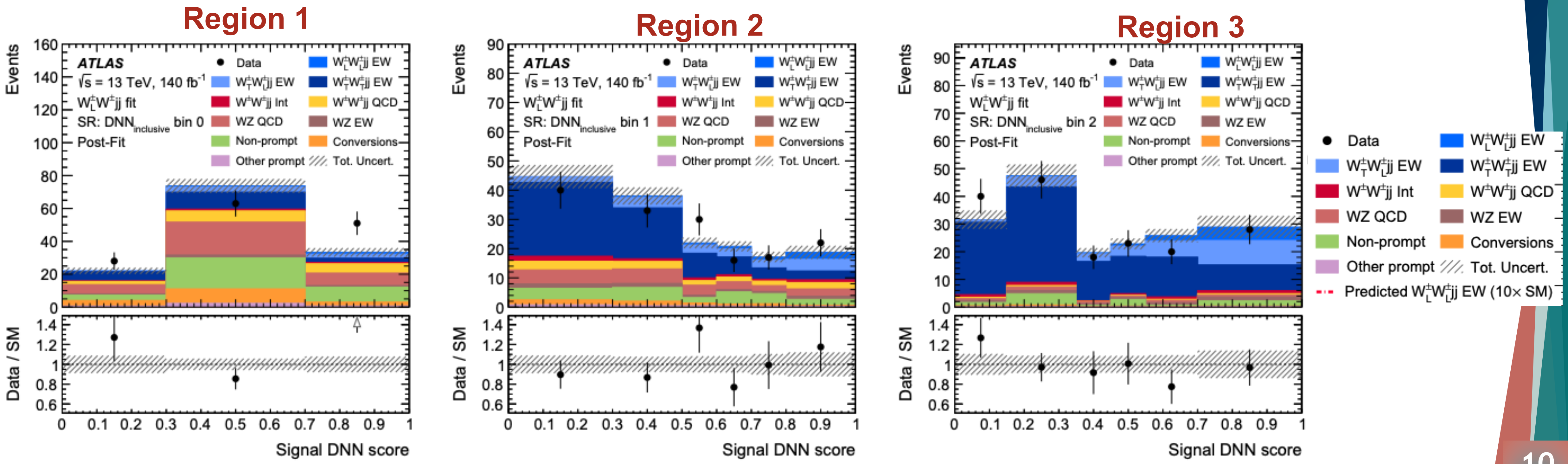

Same-sign W boson polarisation

- Measured fiducial cross-sections times branching fractions are compared to theoretical predictions from Sherpa3
- First fixed-order NLO EW corrections for the different $W_L^{\pm} W_L^{\pm}$ jj, $W_L^{\pm} W_T^{\pm}$jj and $W_T^{\pm}\ W_T^{\pm}$ jj processes are used (arXiv:2409.03620), **reducing by $\approx 15\%$ the cross-section in the SR**

WW centre-of-mass frames

Process	Prediction	Measured $\sigma\mathcal{B}$ (fb)	Uncertainty breakdown (fb)
$W^{\pm}_{\mathrm{L}} W^{\pm}_{\mathrm{L}} jj$	0.29 ± 0.07	0.01 ± 0.21 (tot.)	± 0.20 (stat.) $\pm$ 0.05 (mod. syst.) $\pm$ 0.02 (exp. syst.)
$W^{\pm}_{\mathrm{T}} W^{\pm} jj$	2.56 ± 0.64	3.39 ± 0.35 (tot.)	± 0.30 (stat.) $\pm$ 0.11 (mod. syst.) $\pm$ 0.14 (exp. syst.)
$W^{\pm}_{\mathrm{L}} W^{\pm} jj$	1.18 ± 0.29	0.88 ± 0.30 (tot.)	± 0.28 (stat.) $\pm$ 0.08 (mod. syst.) $\pm$ 0.05 (exp. syst.)
$W^{\pm}_{\mathrm{T}} W^{\pm}_{\mathrm{T}} jj$	1.67 ± 0.40	2.49 ± 0.32 (tot.)	± 0.30 (stat.) $\pm$ 0.09 (mod. syst.) $\pm$ 0.10 (exp. syst.)

partonic centre-of-mass frames

Description	Prediction	Measured $\sigma\mathcal{B}$ (fb)	Uncertainty breakdown (fb)
$W^{\pm}_{\mathrm{L}} W^{\pm}_{\mathrm{L}} jj$	0.19 ± 0.05	0.16 ± 0.22 (tot.)	± 0.21 (stat.) $\pm$ 0.05 (mod. syst.) $\pm$ 0.03 (exp. syst.)
$W^{\pm}_{\mathrm{T}} W^{\pm} jj$	2.67 ± 0.66	3.40 ± 0.35 (tot.)	± 0.31 (stat.) $\pm$ 0.11 (mod. syst.) $\pm$ 0.14 (exp. syst.)
$W^{\pm}_{\mathrm{L}} W^{\pm} jj$	1.24 ± 0.31	0.84 ± 0.37 (tot.)	± 0.35 (stat.) $\pm$ 0.10 (mod. syst.) $\pm$ 0.07 (exp. syst.)
$W^{\pm}_{\mathrm{T}} W^{\pm}_{\mathrm{T}} jj$	1.62 ± 0.39	2.46 ± 0.37 (tot.)	± 0.34 (stat.) $\pm$ 0.10 (mod. syst.) $\pm$ 0.11 (exp. syst.)

Measured cross sections in agreement with the SM predictions

Results driven by the statistical uncertainty of the data in the SR

neutral Triple Gauge Couplings (nTGC) in $Z\gamma$ production

- EW $Z(\rightarrow \ell\ell)\gamma$ production ➔ a powerful test of the SM in the absence of hints of new physics
- nTGC forbidden at the SM tree level:
  - BSM physics could introduce a nTGC vertex
  - SMEFT Dimension-8 or higher operators
- Extension of previous analyses (production XS, differential XS), with a focus on the EFT model
- optimized event selecton for better nTGC sensisitivty on top of the $Z\gamma$ nTGC paper (JHEP 12 (2018) 010) (also full Run2).
- Measured differential cross section as a function of p_T^γ and ϕ_*

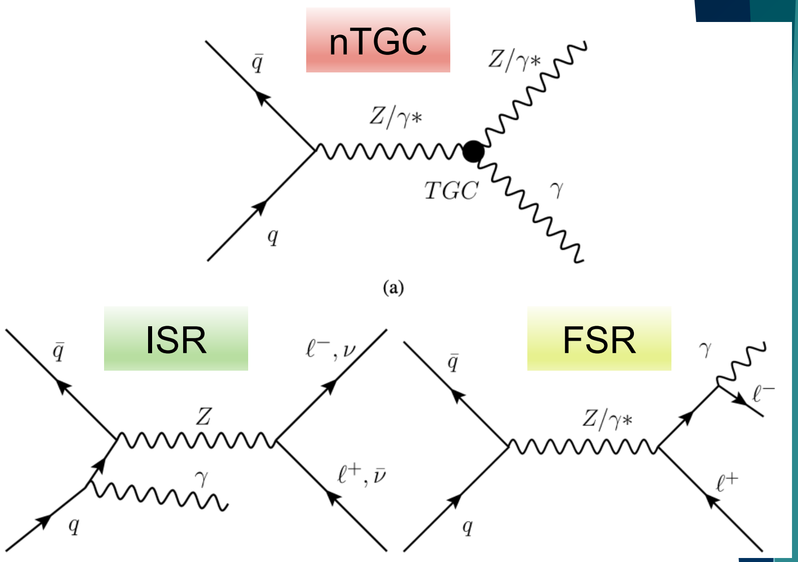

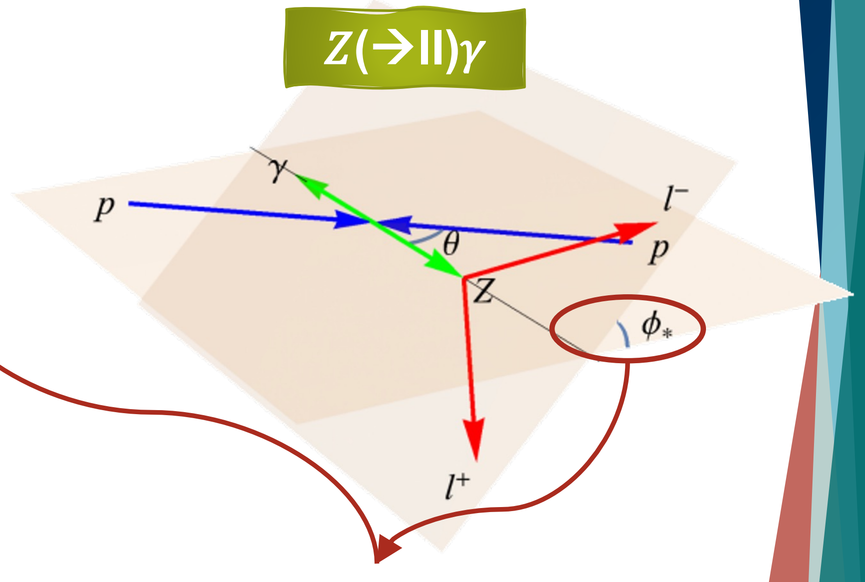

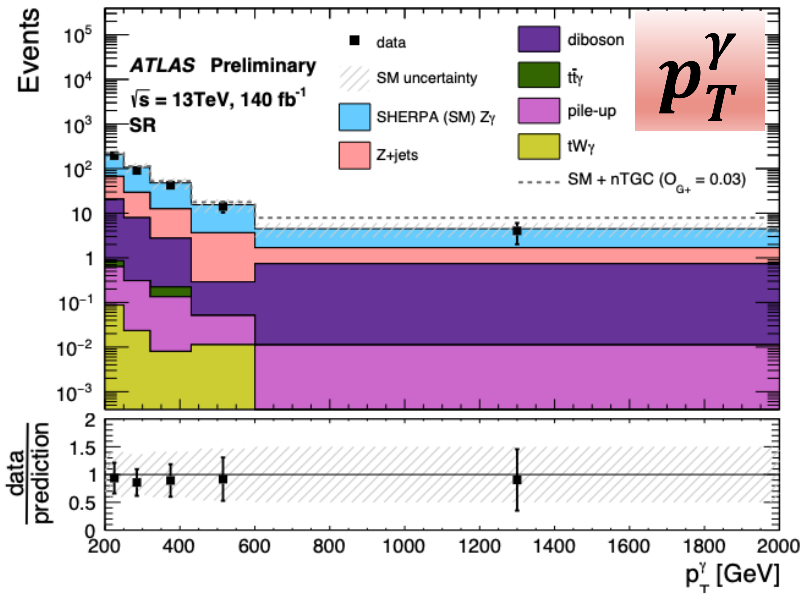

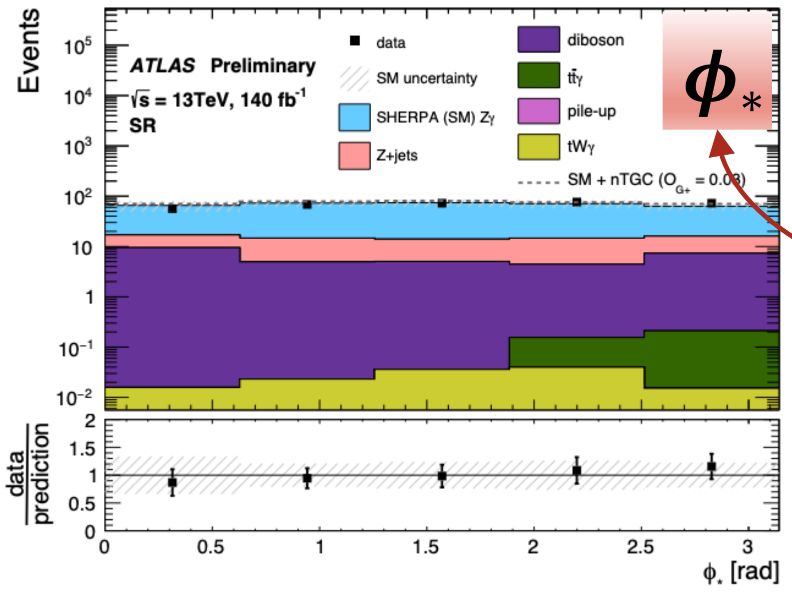

ϕ_* : angle between the scattering and the decay plane of Z boson, in the Z center-of-mass frame

neutral Triple Gauge Couplings (nTGC) in $Z\gamma$ production

- *The theoretical predictions from the calculations of Sherpa 2.2.11 are compared with measurements for p_T^γ and ϕ_* .*
- *Theoretical uncertainties for the predictions are calculated from internal variations of Sherpa sample, including scale variation, PDF variation, uncertainty due to α_S, and EW correction.*

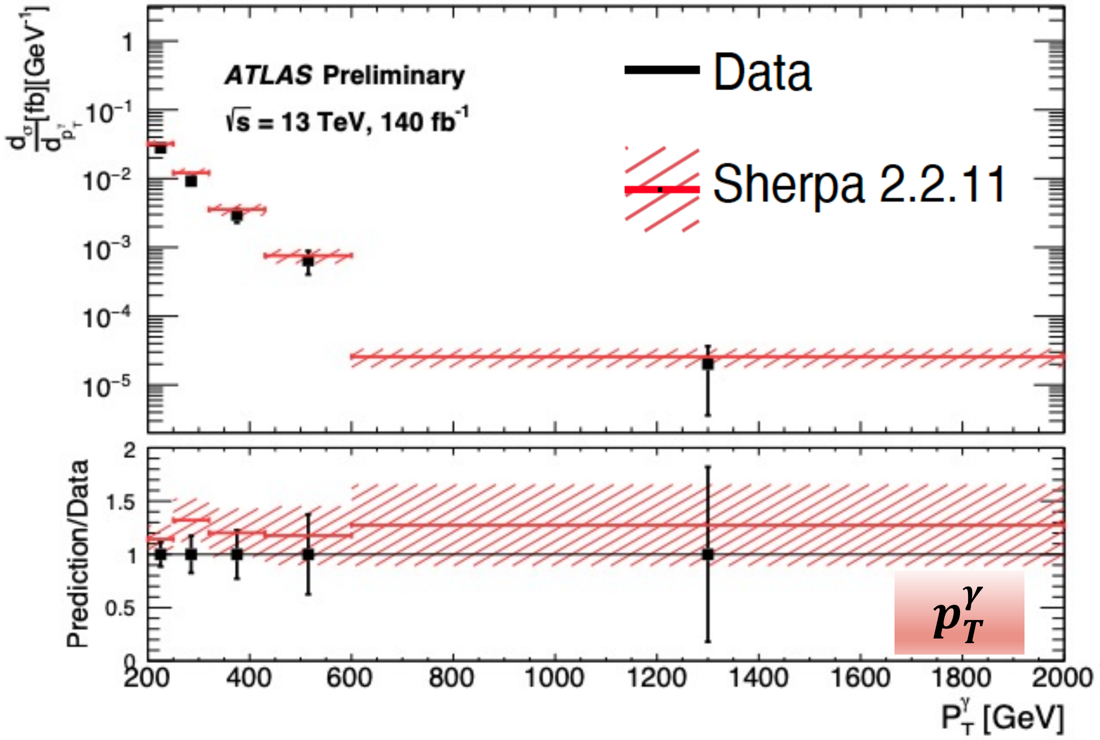

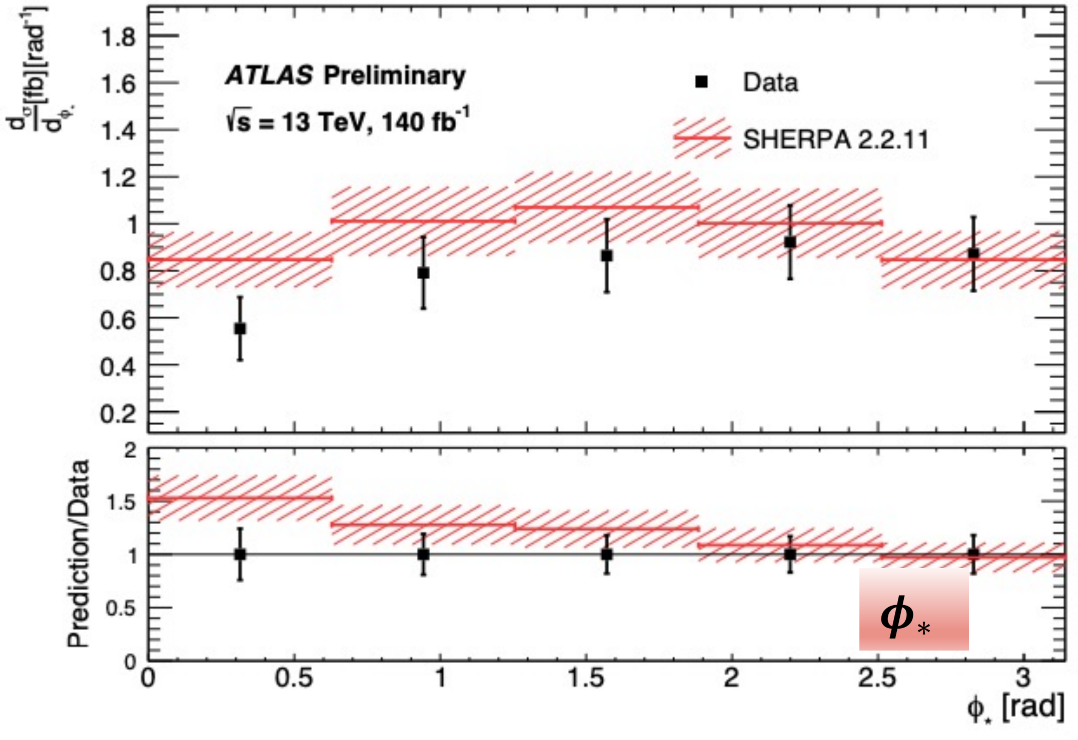

The systematic uncertainties include experimental uncertainties, theoretical uncertainties, and background uncertainties

Source	$ee + \mu\mu$
$Z\gamma$ signal	271.01 ± 2.39 (stat) ± 44.34 (syst)
Z+jets	81.90 ± 71.29 (stat)± 97.65 (syst)
multiboson	33.47 ± 4.58 (stat) ± 10.03 (syst)
pile-up	1.01 ± 0.11 (stat) ± 0.20 (syst)
$t\bar{t}\gamma$	0.31 ± 0.18 (stat) ± 0.05 (syst)
$tW\gamma$	0.13 ± 0.02 (stat) ± 0.04 (syst)
Total prediction	387.83 ± 71.48 (stat) ± 107.71 (syst)
Data	344

Theoretical prediction from Sherpa and data are in agreement within the theoretical uncertainties

neutral Triple Gauge Couplings (nTGC) in Zγ production

Newly generalized form factor formulation for neutral triple gauge vertices

- ($h_3^Z, h_3^\gamma, h_4^\gamma$) map to the effective cutoff scale $\Lambda_i^4 \equiv \frac{\mathcal{O}_i}{\Lambda_i^4}$ where i= G+, G- , B̃W
- Constraints on Wilson coefficients and ***form factors*** ➔ first attempt to incorporate a ***fully gauge-invariant $SU(2)_L \otimes U(1)_Y$ symmetry***
- Superseding former $U(1)_{em}$ only formulation
- New limits on h_4^Z and h_4^γ differ by two orders of magnitude compared to previous ATLAS results due to the updated formulation
- 2D parametrization: interference between two Wilson coefficients taken into account

Wilson coefficients in the SMEFT framework

Parameters	Limits at 95% C.L.	
	Observed 95% C.L.	Expected 95 % C.L.
O_{G+}	[-0.022, 0.020]	[-0.025, 0.023]
O_{G-}	[-1.41, 1.08]	[-1.50, 1.23]
O_{BB}	[-0.37, 0.37]	[-0.44, 0.44]
$O_{\tilde{B}W}$	[-0.54, 0.53]	[-0.62, 0.61]
O_{BW}	[-0.87, 0.95]	[-1.05, 1.14]
O_{WW}	[-1.90, 1.78]	[-2.26, 2.13]

The 95% C.L. limits on two extra dimension-8 operators O_{G+} and O_{G-} parameterized with the fully gauge invariant nTGC formulation are presented for the first time at the LHC

Form factors

Parameters	Limits at 95% C.L.	
	Observed 95% C.L.	Expected 95 % C.L.
h_4^γ	$[-1.3\times10^{-5}, 1.4\times10^{-5}]$	$[-1.5\times10^{-5}, 1.6\times10^{-5}]$
h_4^Z	$[-2.4\times10^{-5}, 2.6\times10^{-5}]$	$[-2.8\times10^{-5}, 3.0\times10^{-5}]$
h_3^γ	$[-3.5\times10^{-4}, 4.6\times10^{-4}]$	$[-4.0\times10^{-4}, 4.9\times10^{-4}]$
h_3^Z	$[-3.2\times10^{-4}, 3.2\times10^{-4}]$	$[-3.7\times10^{-4}, 3.6\times10^{-4}]$

- $s_W = sin\theta_W$
- $c_W = cos\theta_W$
- v = *Higgs field vacuum expectation value*

$$h_3^Z = \frac{1}{[\Lambda_{\tilde{B}W}^4]}\frac{v^2 M_Z^2}{2 s_W c_W} \qquad h_4 = -\frac{1}{[\Lambda_{G+}^4]}\frac{v^2 M_Z^2}{s_W c_W}$$

$$h_3^\gamma = -\frac{1}{[\Lambda_{G-}^4]}\frac{v^2 M_Z^2}{2 c_W^2} \qquad h_4 = \frac{c_W}{s_W} h_4^\gamma$$

More comments in Tobias's talk

Vector Boson Scattering (VBS)

(arXiv: 2503.17461 & SMP-22-011 March 2025)

Vector Boson Scattering: interaction of two vector bosons radiated from the initial-state quarks, yielding a final state with two bosons and two jets, VVjj, in a purely electroweak process

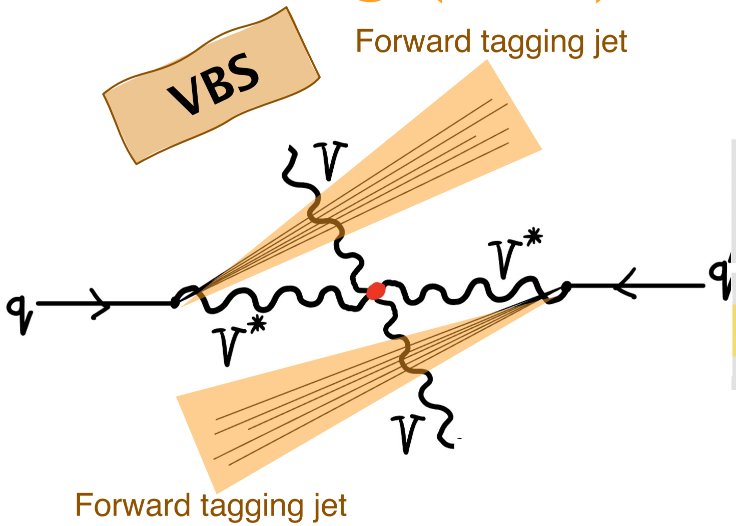

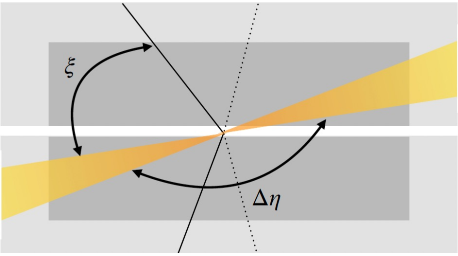

Experimentally challenging due to small xsections (~fb)

EWK production contains both VBS and non-VBS processes → cannot be dissociated

EWK VVJJ VBS

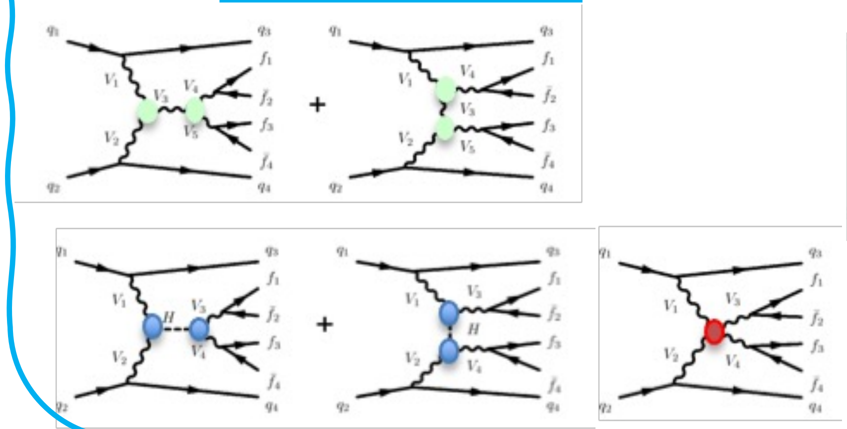

EWK VVJJ NON-VBS

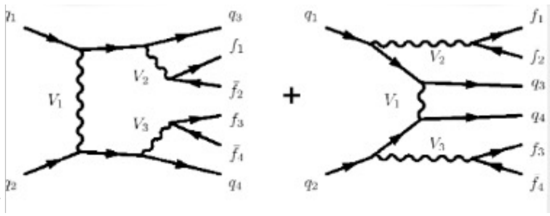

Main background: Diboson QCD production in association with two jets

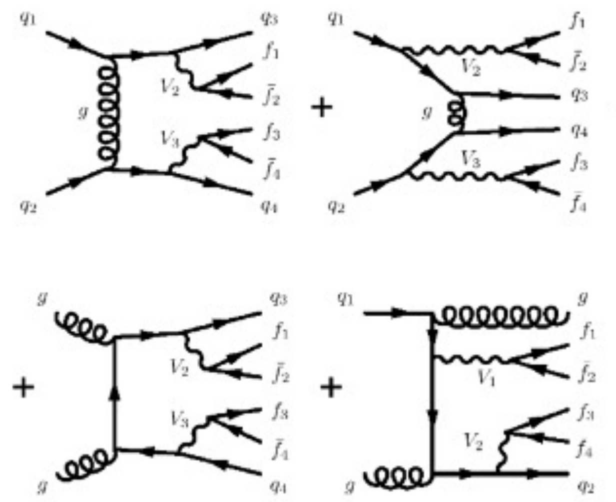

EW diboson production in semileptonic final states at 13 TeV
(arXiv: 2503.17461)

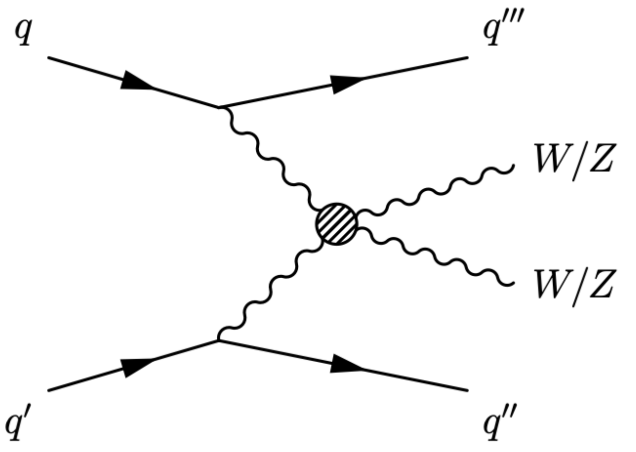

Measurement of semileptonic VBS production at 13 TeV with 140 fb^{-1}

- After **0,1,2 leptons** categorization and **VBS topology tagging jets** require **Hadronic boson decay** (small/large-jets): Merged **or** resolved regions

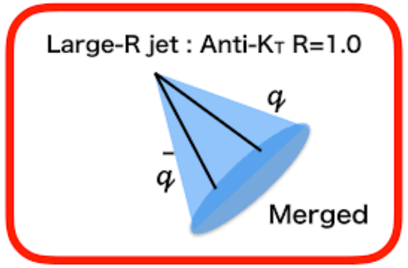

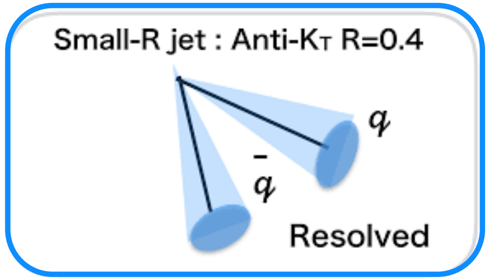

- After **3 Variables Boson tagger** (mass, n_tracks, D_2) designed to provide constant efficiency independent of the jet p_T applied to large-R jets to select those consistent with V→qq 2-prong decays:
  - **Pass 80%** Efficiency boson tagger → **Merged HP**
  - **Pass 50%**, **Fail 80%** Efficiency boson tagger → **Merged LP**
  - **Fail Merged selection** → **Resolved**

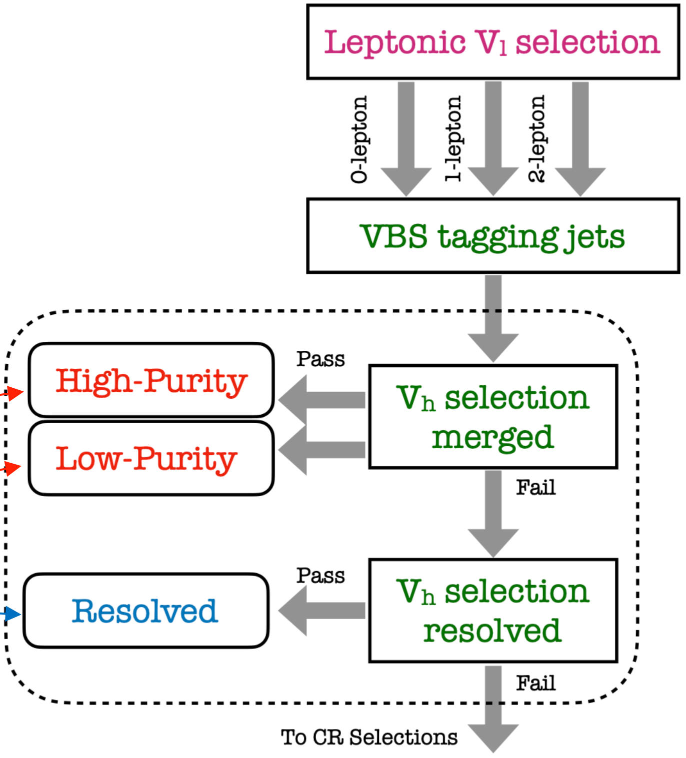

EW diboson production in semileptonic final states at 13 TeV

(arXiv: 2503.17461)

Machine learning approach for final discriminant

A ***Recurrent Neural Network*** **(RNN)** has been developed to separate VBS signal from backgrounds:

- Dedicated training in each channel (0,1,2 leptons) and merged/resolved regions (3x3 SR):
- Low level input jet variables for training: $P_T, \eta, \phi, E, n_{tracks}$
- **RNN score used as final discriminant**

9 SR and 9 CR for V+jets and top background

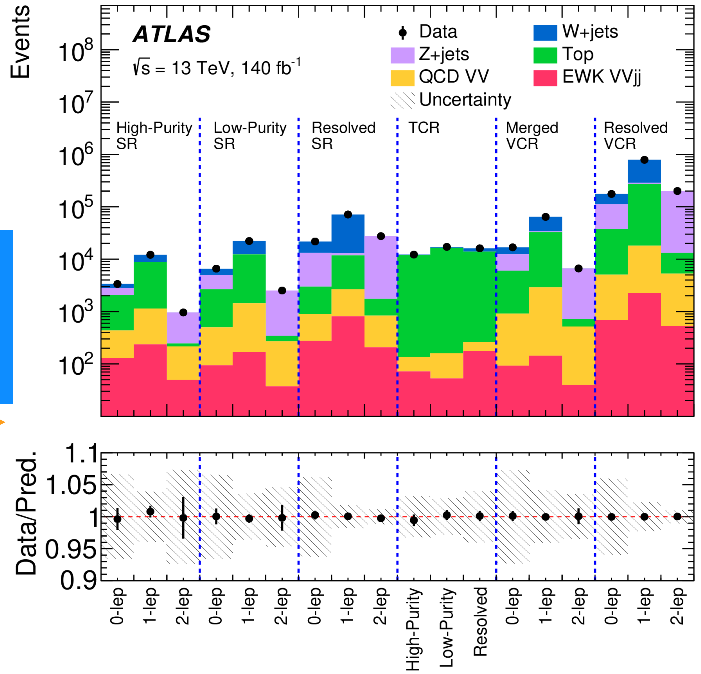

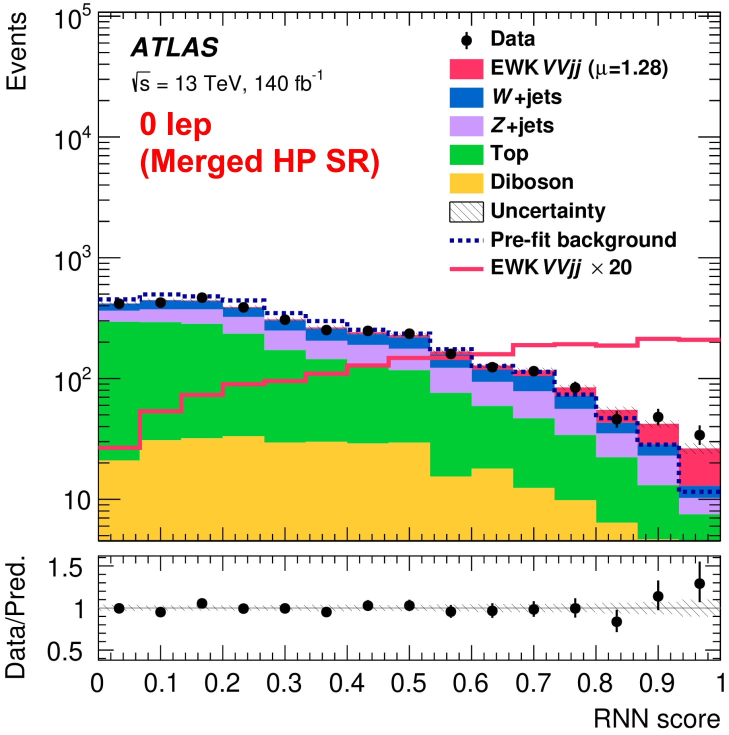

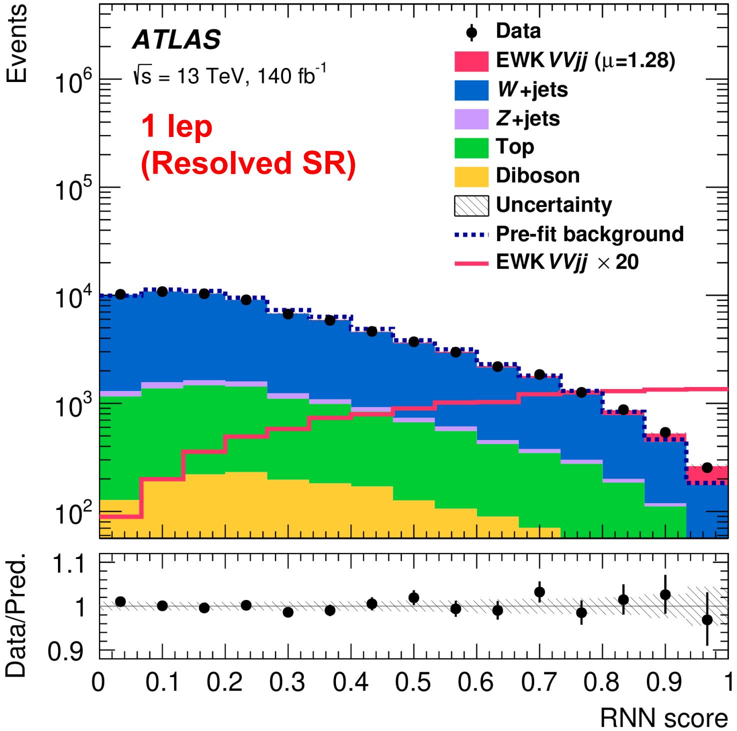

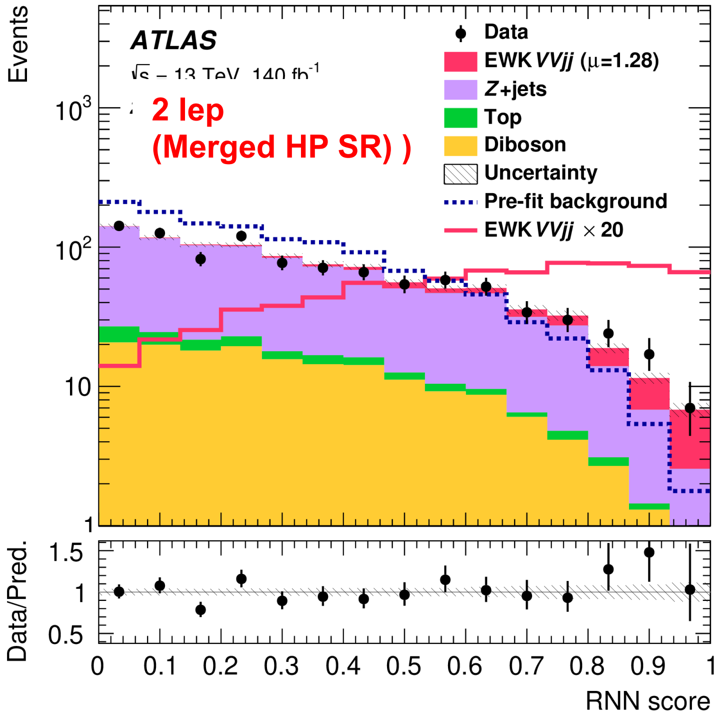

EW diboson production in semileptonic final states at 13 TeV
(arXiv: 2503.17461)

EWK decaying semi-leptonically **observed** with 7.4σ (6.1 expected)

- Measured EW $VVjj$ signal strength:

$$\mu^{\text{obs}}_{\text{EW}} = 1.28^{+0.23}_{-0.21} = 1.28 \pm 0.09\,(\text{stat.})\boxed{{}^{+0.20}_{-0.19}\,(\text{syst.})}$$

Dominated by signal modelling and jet reconstruction uncertainties

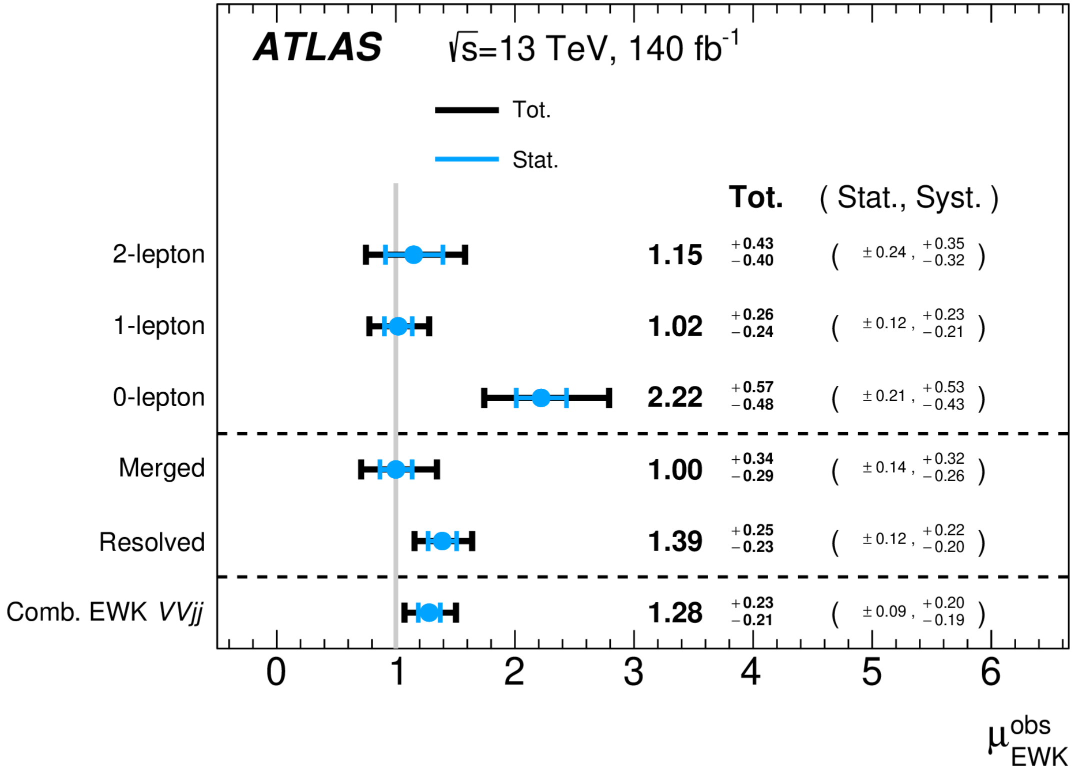

Simultaneously constrain both of EWK and QCD contributions

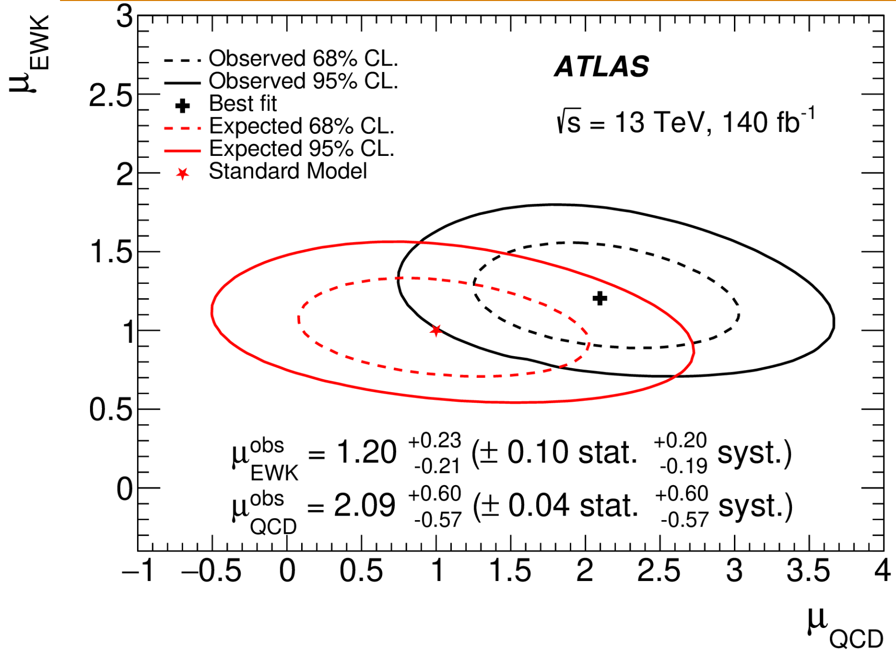

Details on EFT interpretation in Tobias's talk
More details on ATLAS semileptonic VBS analysis in Mathieu's talk

Semileptonic VBS and anomalous quartic gauge couplings

CMS-PAS-SMP-22-011

Measurement of semileptonic VBS production at 13 TeV with **138 fb^{-1}**

- Require **2 leptons** and and **VBS topology tagging jets and Hadronic boson decay** (small/large-jets):

Merged **or** resolved regions

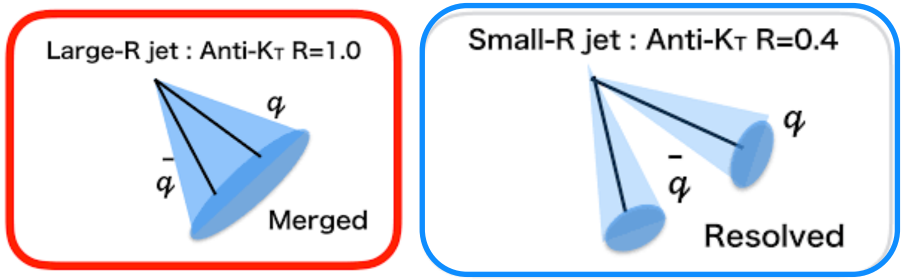

*$\ell\nu qq$ events are used for the EFT combination

4 orthogonal SRs plus CRs to model the main backgrounds (top quark and Drell-Yan)

Machine learning approach for final discriminant

A Deep Neural Network **(DNN)** has been developed to separate VBS signal from backgrounds:

4 SR: Merged/Resolved X **btag**/**b-veto**

Up to 14 input variables used for training, e.g:

m_{jj}, n_{jets} ($p_T > 30$ GeV), ℓ Zeppenfeld, $\Delta\eta_{jj}$

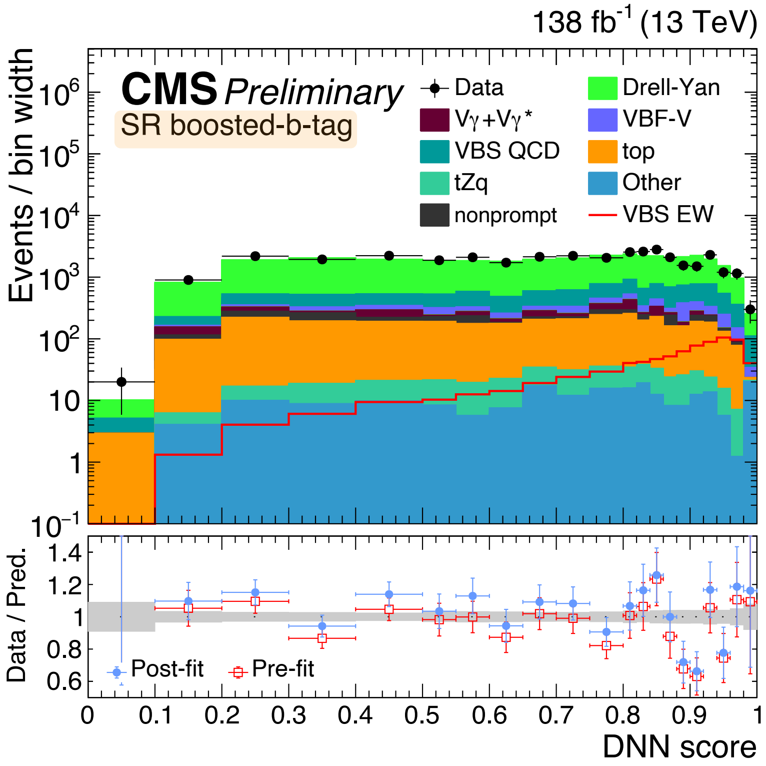

Semileptonic VBS and anomalous quartic gauge couplings

CMS-PAS-SMP-22-011

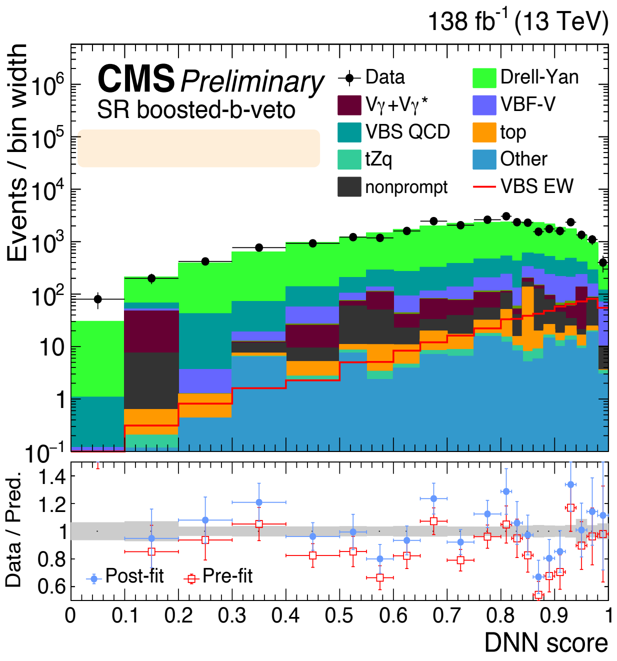

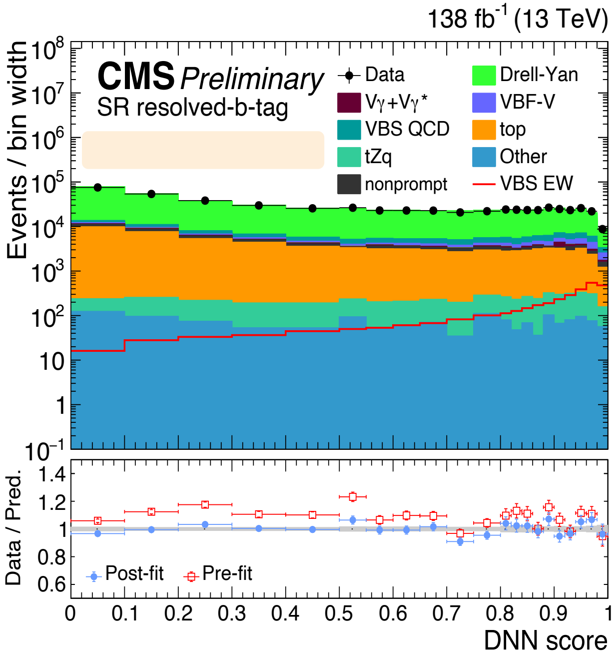

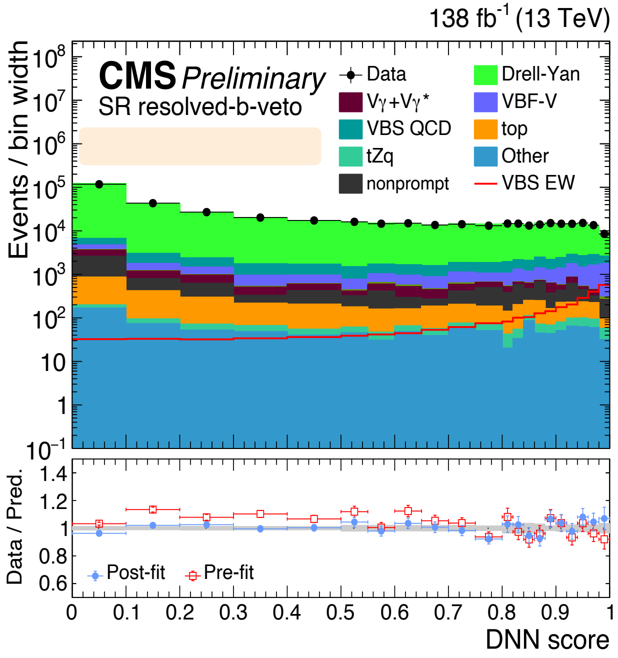

- The obs. (exp.) EW ZV VBS signal strength is

$$\mu_{\mathrm{EW}}^{\mathrm{obs}} = 0.63^{+0.53}_{-0.51} \quad \left(1.00^{+0.61}_{-0.58}\right)$$

Dominated by statistical uncertainty of the data

Impact on $\mu_{\mathrm{EW}}^{\mathrm{obs}}$

Source	$-\Delta\mu$	$+\Delta\mu$
DY and top rate parameters	−0.20	+0.20
Theory	−0.24	+0.26
MC sample size (bin-by-bin unc.)	−0.14	+0.15
Other nuisances	−0.11	+0.13
Data sample size	−0.36	+0.36
Total	−0.51	+0.53

VBS: same-sign W boson scattering in events with one tau lepton

Submitted to J. High Energy Phys. - arXiv:2410.04210

$$pp \rightarrow W^{\pm}W^{\pm}jj \rightarrow \tau^{\pm}\nu_{\tau}\ell^{\pm}\nu_{\ell}\,jj \;\; (\ell = e, \mu)$$

First measurement of the cross section for the scattering of same-sign W boson pairs via the detection of a τ lepton

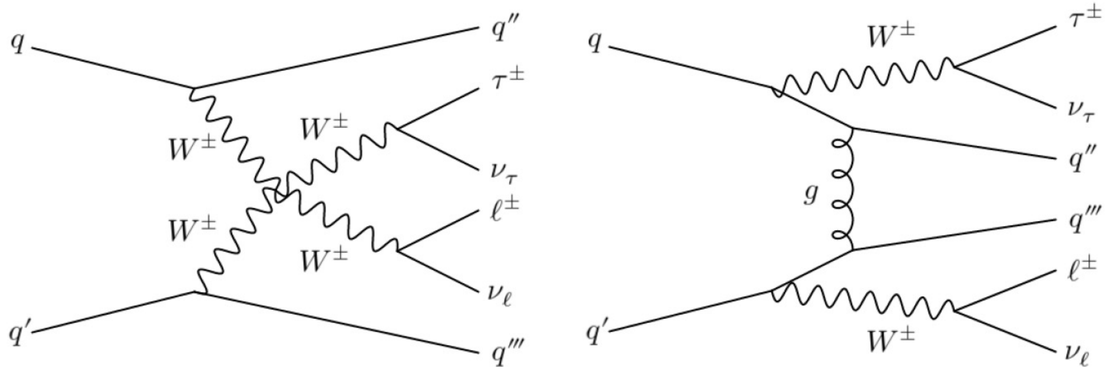

- Events selected if they have two jets with large pseudorapidity and large invariant mass, one τ lepton, one light lepton (e or μ) and significant missing transverse momentum.
- Study of the indirect effects of processes beyond the standard model via the effective field theory framework, in terms of dimension-6 and dimension-8 operators.
- Three **Deep Neural Network Discriminants** (DNNs) to separate to separate the SM VBS (**SM DNN**), EFT dim-6 (**dim-6 DNN**), and EFT dim-8 (**dim-8 DNN**) from the SM background processes.

SM DNN

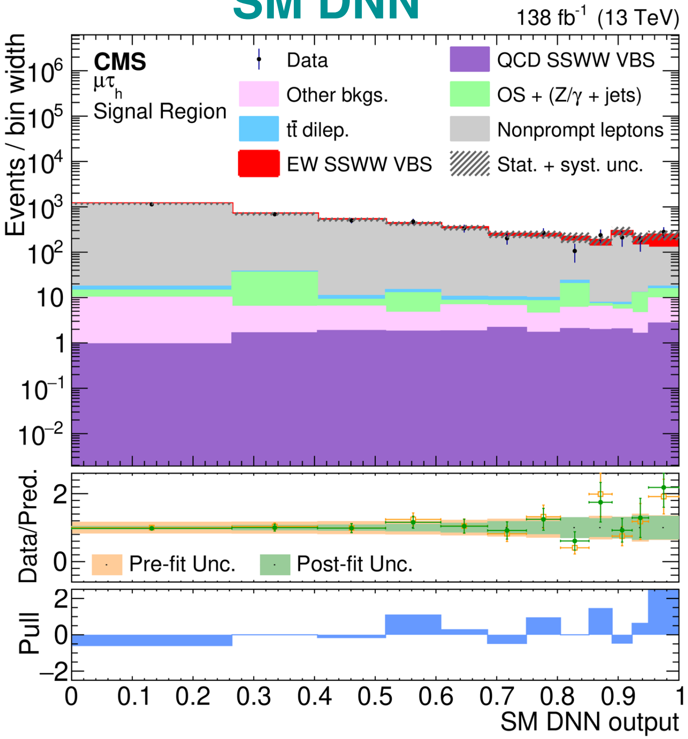

Ratio of the measured cross section for EW same-sign WW scattering and the SM expectations:

$$\frac{\sigma_{\text{measured}}}{\sigma_{\text{SM}}} = 1.44^{+0.63}_{-0.56}$$

Significance of the EW signal: observed 2.7σ - expected 1.9σ

VBS Fully- and semi-leptonic final states combination

$W^{\pm}W^{\pm}$, $W^{\pm}W^{\mp}$, $W^{\pm}Z$, ZZ Combination

CMS-PAS-SMP-24-013

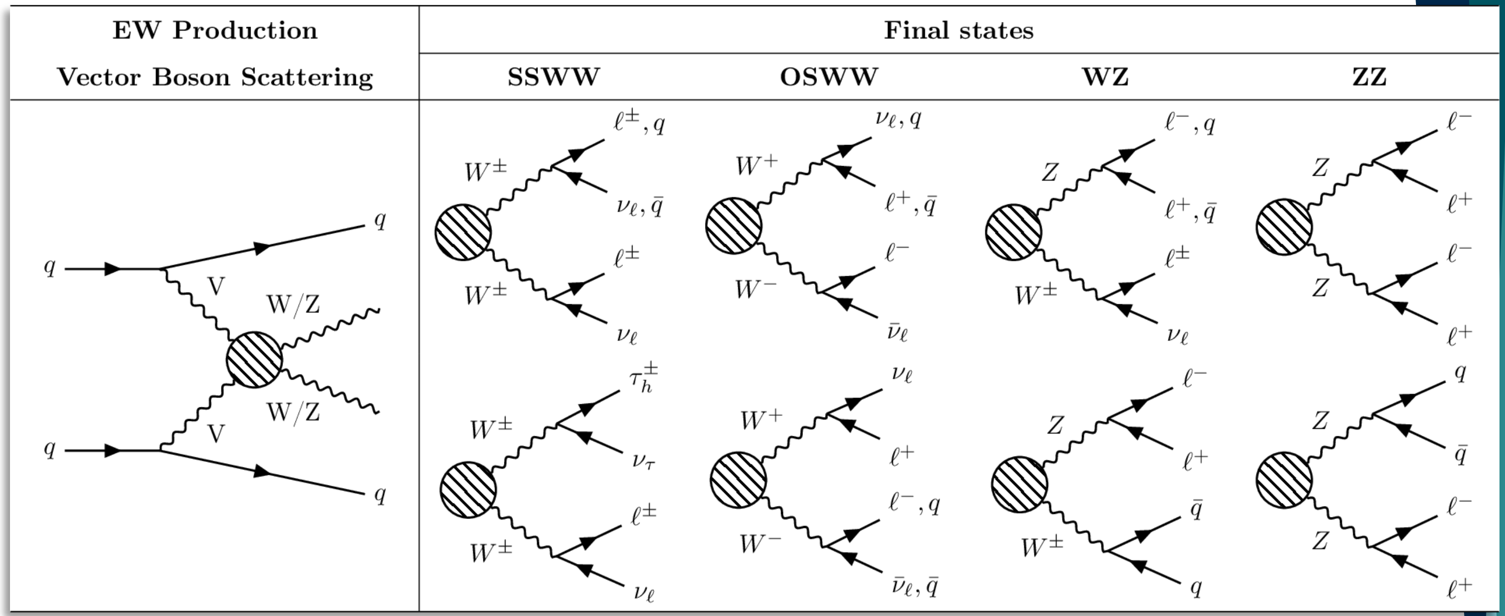

All selected events feature:

- ≥ 2 jets with a high invariant mass and large pseudorapidity separation
- ≥ 1 heavy vector boson decaying leptonically
- Mixed approach using machine learning (DNN, BDT) and traditional variables to separate signal and backgrounds depending on the channel

Two combination models:

- Test Statistic: Profile likelihood ratio $q(\vec{\mu})$
- **4-POIs:** four parameters of interest - signal strengths μ_{OSWW}, μ_{SSWW}, μ_{WZ}, μ_{ZZ}
- **6-POIs:** six parameters of interest - signal strengths $\mu_{W^+W^+}$, $\mu_{W^-W^-}$, $\mu_{W^+W^-}$, μ_{W^+Z}, μ_{W^-Z}, μ_{ZZ}

Test Statistic

$$q(\vec{\mu}) = -2\log\frac{L\left(\vec{x}|\hat{\hat{\vec{\theta}}}\right)}{L\left(\hat{\vec{\mu}}|\hat{\vec{\theta}}\right)}$$

Product of the individual per-channel likelihoods

$$L(\vec{x}|\vec{\mu},\vec{\theta}) = \prod_{\text{bin}=k}\frac{(\vec{\mu}\cdot\vec{s}_k + b_k)^{n_k}}{n_k!}e^{-(\vec{\mu}\cdot\vec{s}_k+b_k)}\cdot\prod_{\text{syst}=j}\pi(\tilde{\theta}_j|\theta_j)$$

- $\hat{\vec{\mu}}$ ➔ the maximum likelihood estimators for the POIs
- $\hat{\vec{\theta}}$ ➔ the maximum likelihood estimators for the nuisance parameters
- $\hat{\hat{\vec{\theta}}}$ ➔ value that maximize the likelihood

VBS Fully- and semi-leptonic final states combination

$W^\pm W^\pm, W^\pm W^\mp, W^\pm Z, ZZ$ Combination

CMS-PAS-SMP-24-013

Two combination models:

- Test Statistic: Profile likelihood ratio
- **4-POIs:** four parameters of interest - signal strengths

  $\mu_{OSWW}, \mu_{SSWW}, \mu_{WZ}, \mu_{ZZ}$

4-POIs	OSWW	SSWW	WZ	ZZ
Observed σ (Expected σ)	6.2 (6.1)	$\gg 5$ ($\gg 5$)	7.0 (5.5)	4.0 (3.6)

- **6-POIs:** six parameters of interest - signal strengths

  $\mu_{W^+W^+}, \mu_{W^-W^-}, \mu_{W^+W^-}, \mu_{W^+Z}, \mu_{W^-Z}, \mu_{ZZ}$

6-POIs	W^+W^-	W^+W^+	W^-W^-	W^+Z	W^-Z	ZZ
Observed σ (Expected σ)	6.1 (6.1)	$\gg 5$ ($\gg 5$)	4.0 (4.6)	5.7 (4.7)	4.2 (3.2)	4.0 (3.6)

results considering four and six independent signal strengths

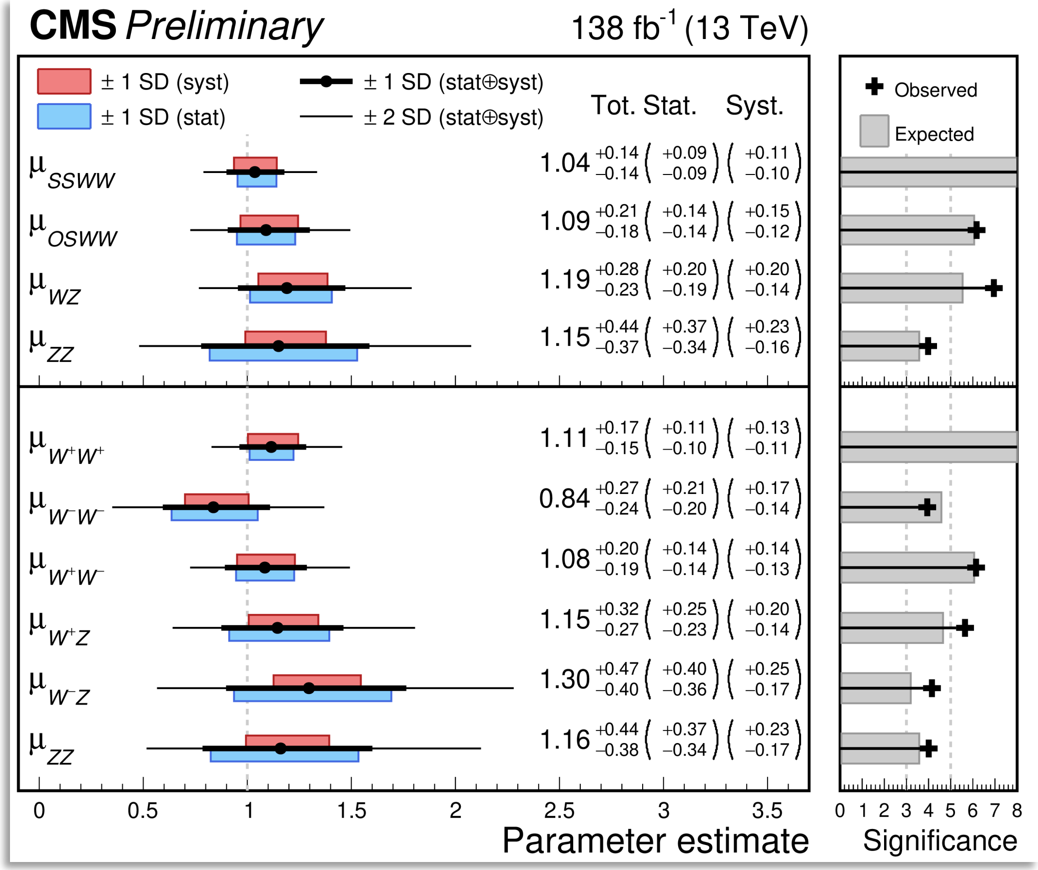

Signal strengths are in agreement with the SM predictions within the 68% CL

VBS fully- and semi-leptonic final states combination

$W^{\pm}W^{\pm}$, $W^{\pm}W^{\mp}$, $W^{\pm}Z$, ZZ Combination

CMS-PAS-SMP-24-013

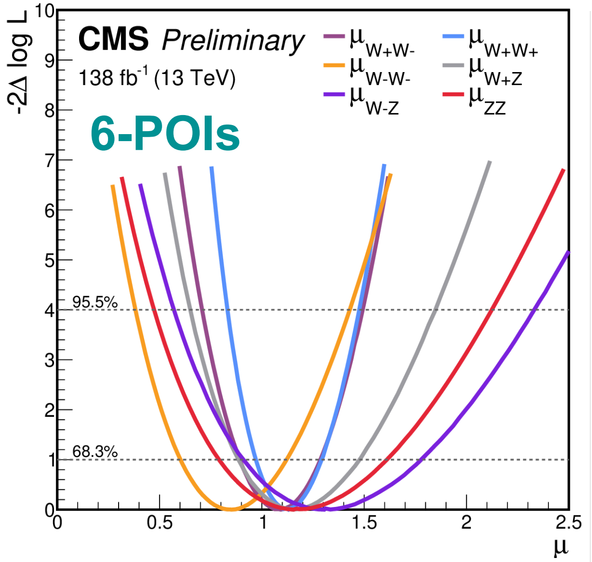

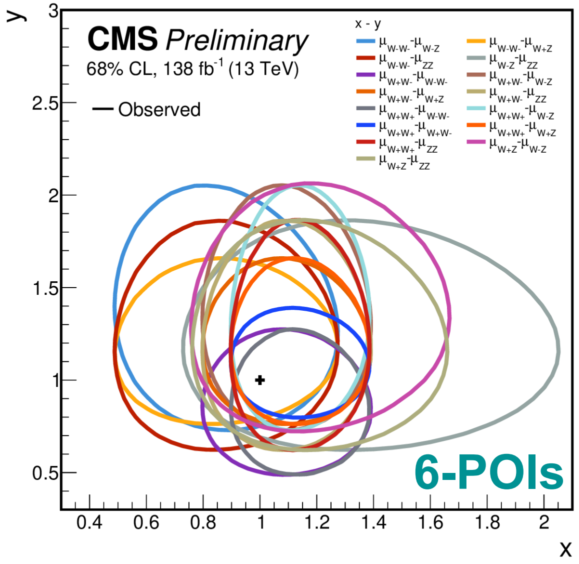

all other POI(s) except the one(s) of interest are profiled in the maximum likelihood fit along with the nuisance parameters.

Simultaneous fits to all pairs of signal strengths are performed to assess the correlation between
the different VBS production modes

Observed $\log_{10}\left(\frac{S(\mu_i=1)}{B}\right)$ *distributions*

for the VBS SM combination and **4-POIs Model**

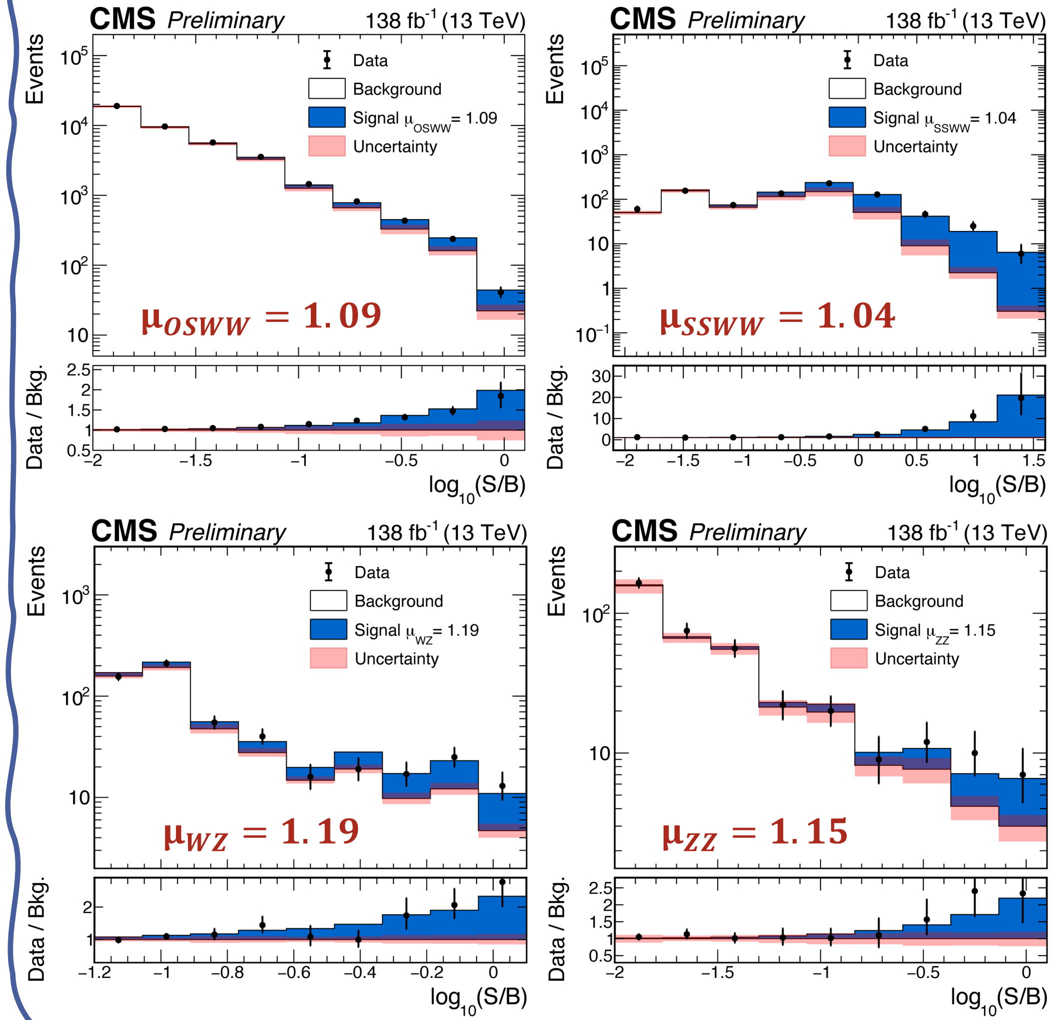

Summary & Conclusions

Recent measurements of diboson production from ATLAS and CMS experiments at $\sqrt{s} = 13\ TeV$ have been presented:

- *Inclusive production cross section measurements of WZ and WW*
- *Same-sign polarisation*
  - First evidence of production of polarised $W_L^{\pm}W^{\pm}$: observed significance **3.3σ**, with a measured cross-section of $\mathbf{0.88 \pm 0.30\ fb}$
  - Most stringent limits to date for the cross-section of $W_L^{\pm}W_L^{\pm}$: observed 95% CL upper limit of $\mathbf{0.45\ fb}$ (expected 0.70 fb)
- *EW diboson production in semileptonic and fully hadronic final states*
  - EWK decaying semi-leptonically observed with **7.4σ (6.1 expected)**
  - ATLAS and CMS reported improvements on aQGCs upper limits
  - First measurement of the cross section for the scattering of same-sign W boson pairs via the detection of a τ lepton $\frac{\sigma_{measured}}{\sigma_{SM}} = \mathbf{1.44^{+0.63}_{-0.56}}$
  - First Combination of fully- and semi-leptonic final states

Backup

Inclusive WZ production cross section

Submitted to J. High Energy Phys. - arXiv:2412.02477

Table 1: Requirements for the definition of the signal and control regions of the analysis. Objects in parentheses relate to the ZZ CR.

Region	N_ℓ	$p_T\{\ell_Z^1, \ell_Z^2, \ell_W(\ell_3), (\ell_4)\}$ (GeV)	N_{OSSF}	$\lvert m(\ell_Z^1, \ell_Z^2) - m_Z \rvert$ (GeV)	p_T^{miss} (GeV)	$N_{b\,tag}$	$\min(m(\ell, \ell'))$ (GeV)	$m(\ell_Z^1, \ell_Z^2, \ell_W(\ell_3))$ (GeV)
SR	=3	>{25, 15, 25}	≥1	<15	>35	=0	>4	>100
ZZ CR	=4	>{25, 15, 25, 15}	≥1	<15	—	=0	>4	>100
$t\bar{t}$Z CR	=3	>{25, 15, 25}	≥1	<15	>35	>0	>4	>100
Xγ CR	=3	>{25, 15, 25}	≥1	—	≤35	=0	>4	<100

Fiducial and Total regions

Region	Fiducial	Total
Lepton definition	Dressed (e, μ)	Dressed (e, μ, τ)
$N_\ell = 3$	✓	✓
$p_T\{\ell_Z^1, \ell_Z^2, \ell_W\} > \{25, 15, 25\}$ GeV	✓	—
$\lvert\eta\rvert\{\ell_Z^1, \ell_Z^2, \ell_W\} < \{2.5, 2.5, 2.5\}$	✓	—
$N_{OSSF} = 1$	✓	✓
$\lvert m(\ell_Z^1, \ell_Z^2) - m_Z\rvert < 30$ GeV	✓	✓
$\min(m(\ell, \ell')) > 4$ GeV	✓	✓
$m(\ell_Z^1, \ell_Z^2, \ell_W) > 100$ GeV	✓	—

p_T of one of the leptons arising from the Z in the 3 CRs

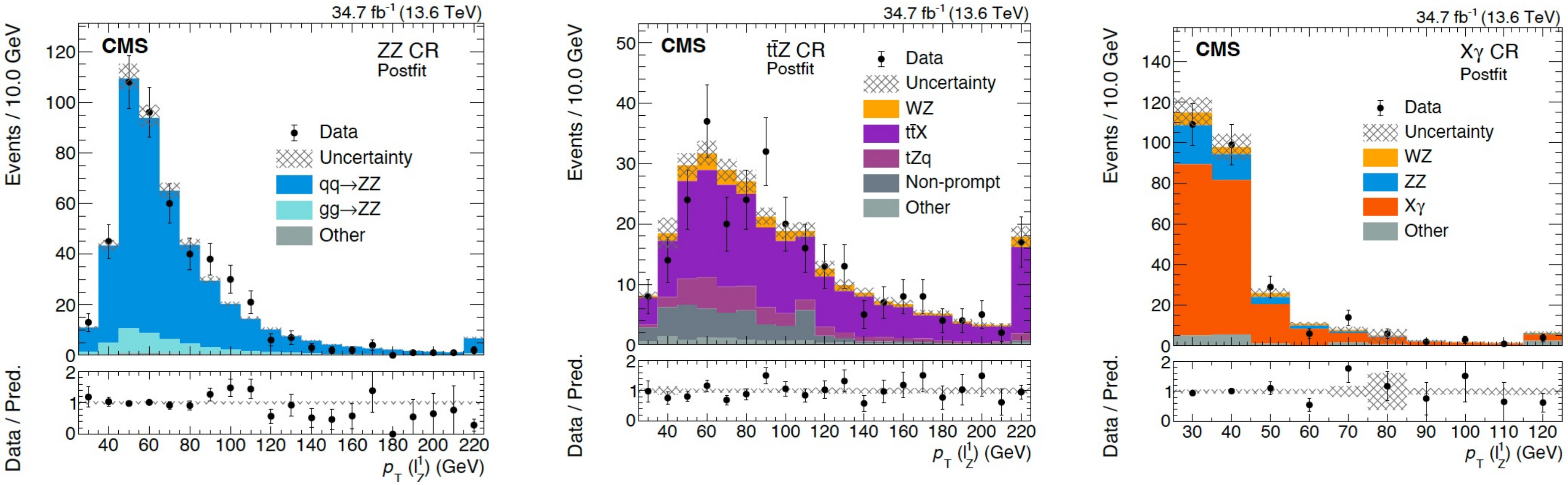

selected events

Process	eee	eeμ	$\mu\mu$e	$\mu\mu\mu$	Inclusive
Non-prompt	25 ± 7	13 ± 5	24 ± 7	30 ± 10	93 ± 15
ZZ	25 ± 2	37 ± 1	49 ± 3	75 ± 3	186 ± 5
Xγ	12 ± 2	2.5 ± 0.3	24 ± 2	3.2 ± 0.5	41 ± 3
$t\bar{t}$X	8.0 ± 0.8	11 ± 1	14 ± 1	21 ± 2	54 ± 3
VVV	4 ± 1	5 ± 2	7 ± 3	10 ± 4	27 ± 5
VH	3.0 ± 0.5	3.8 ± 0.7	5 ± 1	9 ± 2	20 ± 2
tZq	4.2 ± 0.5	5.3 ± 0.6	7.5 ± 0.9	11 ± 1	28 ± 2
Background	82 ± 8	78 ± 5	130 ± 9	160 ± 11	450 ± 17
WZ	410 ± 10	556 ± 12	768 ± 14	1096 ± 22	2830 ± 31
Prediction	491 ± 13	634 ± 13	898 ± 16	1256 ± 24	3280 ± 34
Data	491	643	869	1276	3279

Inclusive WZ production cross section

Submitted to J. High Energy Phys. - arXiv:2412.02477

Source	Inclusive (%)	eee (%)	$ee\mu$ (%)	$\mu\mu e$ (%)	$\mu\mu\mu$ (%)
Integrated luminosity	1.5	1.5	1.4	1.4	1.5
Trigger efficiencies	0.5	1.0	1.0	1.0	0.7
b tagging	0.1	0.1	0.1	0.1	0.1
Pileup	0.4	0.6	0.8	0.2	0.4
Jet energy scales	0.9	1.3	0.7	1.1	0.7
Electron reconstruction	1.2	4.0	2.9	1.1	—
Electron ident. efficiencies	0.7	3.6	2.4	1.1	—
Electron energy scale	0.1	0.1	0.1	0.0	—
Muon efficiencies	0.7	—	0.3	0.8	1.2
Non-prompt bkg. normalization	0.7	1.6	0.5	0.7	0.7
VVV normalization	0.4	0.4	0.4	0.4	0.4
tZq normalization	0.1	0.1	0.1	0.1	0.1
ZZ normalization	0.3	0.8	0.7	0.5	0.5
$t\bar{t}Z$ normalization	0.3	0.7	0.6	0.4	0.5
$X\gamma$ normalization	0.2	0.7	0.3	0.4	0.2
VH normalization	0.2	0.2	0.2	0.1	0.2
ISR/FSR	0.3	0.5	0.2	0.4	0.3
WZ theory (μ_R, μ_F, PDF)	0.2	0.2	0.2	0.2	0.2
MC statistical	0.5	1.9	0.9	1.0	0.9
Statistical	2.0	5.3	4.6	3.8	3.3
Total	3.3	8.4	6.4	5.0	4.2

Category	Accuracy	Fiducial cross section (fb)
eee	POWHEG, NLO QCD	$68.0^{+2.3}_{-2.1}$ (scale) $\pm$ 1.0 (PDF)
	MATRIX, NLO QCD	$69.9^{+3.9}_{-3.1}$ (scale)
	MATRIX, NNLO QCD	$77.0^{+1.8}_{-1.7}$ (scale)
	MATRIX, NNLO QCD $\times$ NLO EW	$75.4^{+1.7}_{-1.6}$ (scale)
	Measured	72.0 $\pm$ 4.0 (stat) $\pm$ 4.5 (syst) $\pm$ 1.0 (lumi) $\pm$ 0.1 (theo)
$ee\mu$	POWHEG, NLO QCD	$68.0^{+2.3}_{-2.1}$ (scale) $\pm$ 1.0 (PDF)
	MATRIX, NLO QCD	$68.7^{+3.8}_{-3.0}$ (scale)
	MATRIX, NNLO QCD	$75.0^{+1.8}_{-1.6}$ (scale)
	MATRIX, NNLO QCD $\times$ NLO EW	$73.4^{+1.7}_{-1.5}$ (scale)
	Measured	73.9 $\pm$ 3.5 (stat) $\pm$ 3.1 (syst) $\pm$ 1.1 (lumi) $\pm$ 0.3 (theo)
$\mu\mu e$	POWHEG, NLO QCD	$68.0^{+2.3}_{-2.1}$ (scale) $\pm$ 1.0 (PDF)
	MATRIX, NLO QCD	$68.7^{+3.8}_{-3.0}$ (scale)
	MATRIX, NNLO QCD	$75.0^{+1.8}_{-1.6}$ (scale)
	MATRIX, NNLO QCD $\times$ NLO EW	$73.4^{+1.7}_{-1.5}$ (scale)
	Measured	71.2 $\pm$ 2.9 (stat) $\pm$ 2.0 (syst) $\pm$ 1.0 (lumi) $\pm$ 0.1 (theo)
$\mu\mu\mu$	POWHEG, NLO QCD	$68.0^{+2.3}_{-2.1}$ (scale) $\pm$ 1.0 (PDF)
	MATRIX, NLO QCD	$69.9^{+3.9}_{-3.1}$ (scale)
	MATRIX, NNLO QCD	$77.0^{+1.8}_{-1.7}$ (scale)
	MATRIX, NNLO QCD $\times$ NLO EW	$75.4^{+1.7}_{-1.6}$ (scale)
	Measured	75.3 $\pm$ 2.5 (stat) $\pm$ 1.5 (syst) $\pm$ 1.1 (lumi) $\pm$ 0.1 (theo)
Inclusive	POWHEG, NLO QCD	$271.9^{+9.0}_{-8.5}$ (scale) $\pm$ 3.8 (PDF)
	MATRIX, NLO QCD	$277.1^{+15.3}_{-12.3}$ (scale)
	MATRIX, NNLO QCD	$304.0^{+7.1}_{-6.6}$ (scale)
	MATRIX, NNLO QCD $\times$ NLO EW	$298.1^{+6.9}_{-6.3}$ (scale)
	Measured	297.6 $\pm$ 6.4 (stat) $\pm$ 6.4 (syst) $\pm$ 4.2 (lumi) $\pm$ 0.5 (theo)

Inclusive WW and differential cross section

Accepted by Phys. Lett. B. - arXiv:2406.05101

Table 1: Summary of the requirements defining the WW SR and dilepton CRs.

Quantity	WW	One/two b tags	$Z \to \tau\tau$	Same-sign
Number of tight leptons	Strictly 2			
Additional loose leptons	0			
Lepton charges	Opposite			Same
$p_T^{\ell\,\max}$	>25 GeV			
$p_T^{\ell\,\min}$	>20 GeV			
$m_{\ell\ell}$	>85 GeV	>85 GeV	<85 GeV	>85 GeV
$p_T^{\ell\ell}$	—	—	<30 GeV	—
Number of b-tagged jets	0	1/2	0	0
N_j	$0/1/2/\geq 3$			

	WW SR	Same-sign CR	$Z \to \tau\tau$ CR	One b tag CR	Two b tags CR
Data	43 898	3 456	56 551	68 656	57 617
WW	$16\,030 \pm 160$	80.9 ± 5.0	$2\,648 \pm 37$	$2\,128 \pm 27$	227 ± 11
Top quark	$19\,900 \pm 130$	87.9 ± 3.7	$1\,131.6 \pm 8.8$	$63\,450 \pm 210$	$55\,550 \pm 210$
$Z \to \tau\tau$	$2\,124 \pm 31$	57.1 ± 4.1	$45\,610 \pm 320$	226.0 ± 8.6	19.5 ± 2.3
WZ	487.7 ± 8.6	512.1 ± 9.6	97.6 ± 2.1	97.1 ± 2.1	11.8 ± 0.6
ZZ	37.1 ± 0.8	33.6 ± 0.7	66.0 ± 1.6	6.9 ± 0.2	1.0 ± 0.0
Nonprompt	$4\,880 \pm 140$	$2\,390 \pm 53$	$6\,580 \pm 280$	$2\,670 \pm 100$	$1\,695 \pm 98$
VVV	76.0 ± 1.6	25.8 ± 0.6	4.7 ± 0.1	33.7 ± 1.1	8.6 ± 0.4
tVx	10.7 ± 0.5	8.7 ± 1.1	0.7 ± 0.1	44.1 ± 1.4	52.0 ± 1.6
$V\gamma$	226.5 ± 7.7	233.3 ± 7.5	68.8 ± 3.4	43.4 ± 3.4	3.0 ± 0.4
Higgs boson	90.2 ± 6.4	27.2 ± 1.7	345 ± 32	29.4 ± 1.7	20.9 ± 1.2
Total	$43\,860 \pm 180$	$3\,457 \pm 53$	$56\,550 \pm 240$	$68\,720 \pm 220$	$57\,590 \pm 230$

	WZ CR	ZZ CR
Data	4 732	610
WZ	$3\,470 \pm 85$	0.9 ± 0.1
ZZ	271 ± 20	599 ± 25
Nonprompt	819 ± 80	< 1
VVV	60.5 ± 2.9	5.4 ± 0.2
tVx	26.0 ± 2.3	2.3 ± 0.2
$V\gamma$	55.8 ± 6.0	< 1
Higgs boson	28.4 ± 1.9	2.4 ± 0.6
Total	$4\,729 \pm 76$	610 ± 25

Table 2: Summary of the requirements defining the WZ and ZZ CRs.

Variable	WZ	ZZ
Number of tight leptons	Strictly 3	Strictly 4
Additional loose leptons	0	
Lepton p_T	>25/10/20 GeV	>25/20/10/10 GeV (p_T ordered)
$\|m_{\ell\ell} - m_Z\|$	<15 GeV	<15 GeV (both pairs)
$m_{3\ell}$	>100 GeV	—
$m_{4\ell}$	—	>150 GeV
p_T^{miss}	>30 GeV	—
Number of b-tagged jets	0	

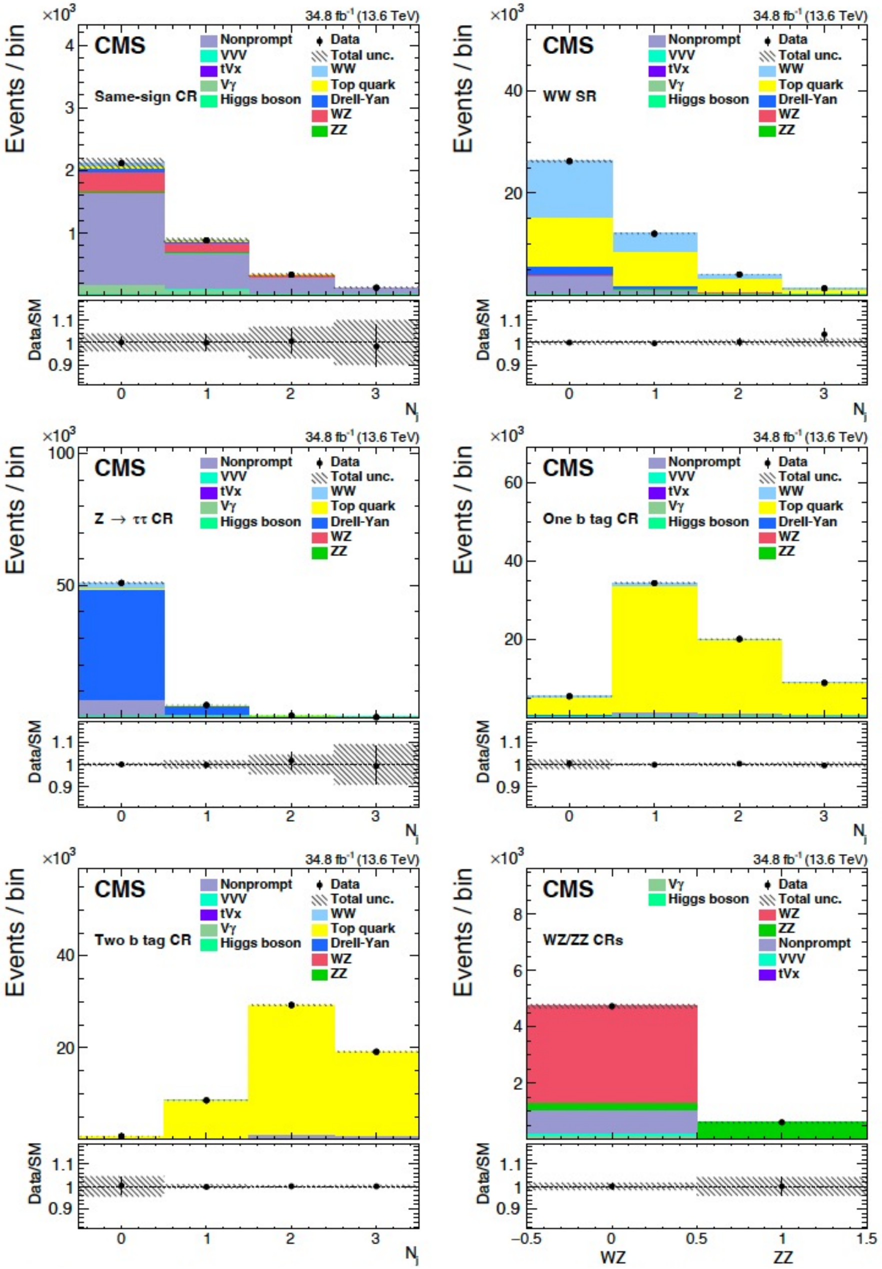

Inclusive WW and differential cross section

Accepted by Phys. Lett. B. - arXiv:2406.05101

Table 4: Definition of the fiducial region.

Variable	Requirement
Lepton origin	Direct decay of a prompt W boson
Lepton definition	Dressed leptons ($e^{\pm}\mu^{\mp}$)
Leading lepton p_T	$p_T^{\ell\,\max} > 25\,\mathrm{GeV}$
Trailing lepton p_T	$p_T^{\ell\,\min} > 20\,\mathrm{GeV}$
Additional leptons	0
$\lvert\eta\rvert$ of leptons	$\lvert\eta\rvert < 2.5$
Dilepton mass	$m_{\ell\ell} > 85\,\mathrm{GeV}$
Jet p_T	$p_T^{j} > 30\,\mathrm{GeV}$
$\lvert\eta\rvert$ of jets	$\lvert\eta^{j}\rvert < 2.5$
Jet-lepton removal	$\Delta R(j,\ell) > 0.4$

Table 7: Inclusive fiducial cross section and normalized cross sections for events with $N_j = 0, 1, \geq 2$ jets. The uncertainty listed is the total uncertainty obtained from the fit to the yields. The expected predictions are obtained from POWHEG+PYTHIA. In parentheses, the split of systematic and statistical uncertainties are reported.

Observable	Expected	Observed
Cross section (fb)	$812 \pm 34\,(31, 15)$	$813 \pm 35\,(32, 15)$
0-jet fraction	$0.648 \pm 0.015\,(0.012, 0.009)$	$0.640 \pm 0.016\,(0.013, 0.009)$
1-jet fraction	$0.256 \pm 0.013\,(0.008, 0.010)$	$0.243 \pm 0.013\,(0.009, 0.010)$
$\geq$2-jet fraction	$0.096 \pm 0.011\,(0.008, 0.008)$	$0.119 \pm 0.011\,(0.008, 0.008)$

Search for neutral triple gauge couplings (nTGC) and measurement of Z(->ll)y

Quantity	Cuts
lepton kinematics	$p_T(\ell_1) > 30$ GeV, $p_T(\ell_2) > 25$ GeV, $\lvert\eta\rvert < 2.47$
photon kinematics	$p_T^\gamma > 200$ GeV, $\lvert\eta\rvert < 2.37$, $\Delta R(\gamma, \ell) > 0.4$
photon isolation	$E_T^{\text{cone20}}/E_T^\gamma < 0.07$
jet kinematics	$p_T(j) > 30$ GeV if $\lvert\eta\rvert < 2.5$ or $p_T(j) > 50$ GeV if $2.5 < \lvert\eta\rvert < 4.5$
invariant mass	$\lvert m_{\ell\ell} - m_Z\rvert < 10$ GeV, $(m_{\ell\ell} + m_{\ell\ell\gamma}) > 182$ GeV
jet multiplicity	$N_{\text{jet}} = 0$

Table 4: Definition of the fiducial region at particle level.

Source	$ee + \mu\mu$
$Z\gamma$ signal	271.01 ± 2.39 (stat) ± 44.34 (syst)
Z+jets	81.90 ± 71.29 (stat)± 97.65 (syst)
multiboson	33.47 ± 4.58 (stat) ± 10.03 (syst)
pile-up	1.01 ± 0.11 (stat) ± 0.20 (syst)
$t\bar{t}\gamma$	0.31 ± 0.18 (stat) ± 0.05 (syst)
$tW\gamma$	0.13 ± 0.02 (stat) ± 0.04 (syst)
Total prediction	387.83 ± 71.48 (stat) ± 107.71 (syst)
Data	344

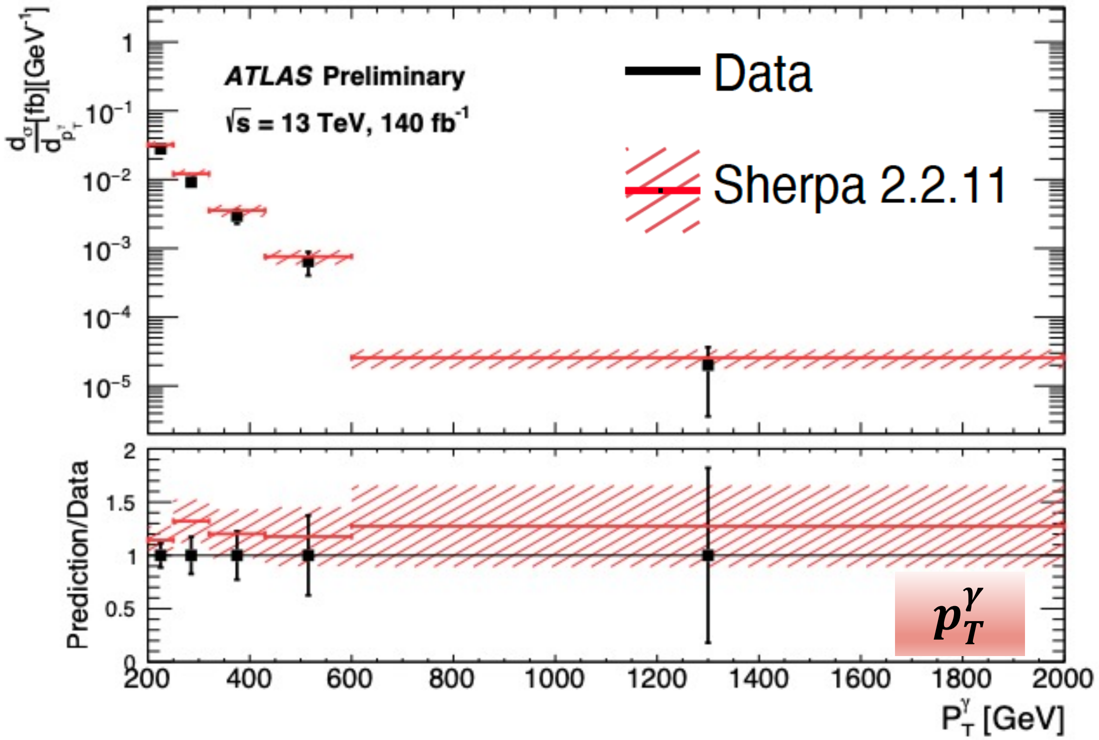

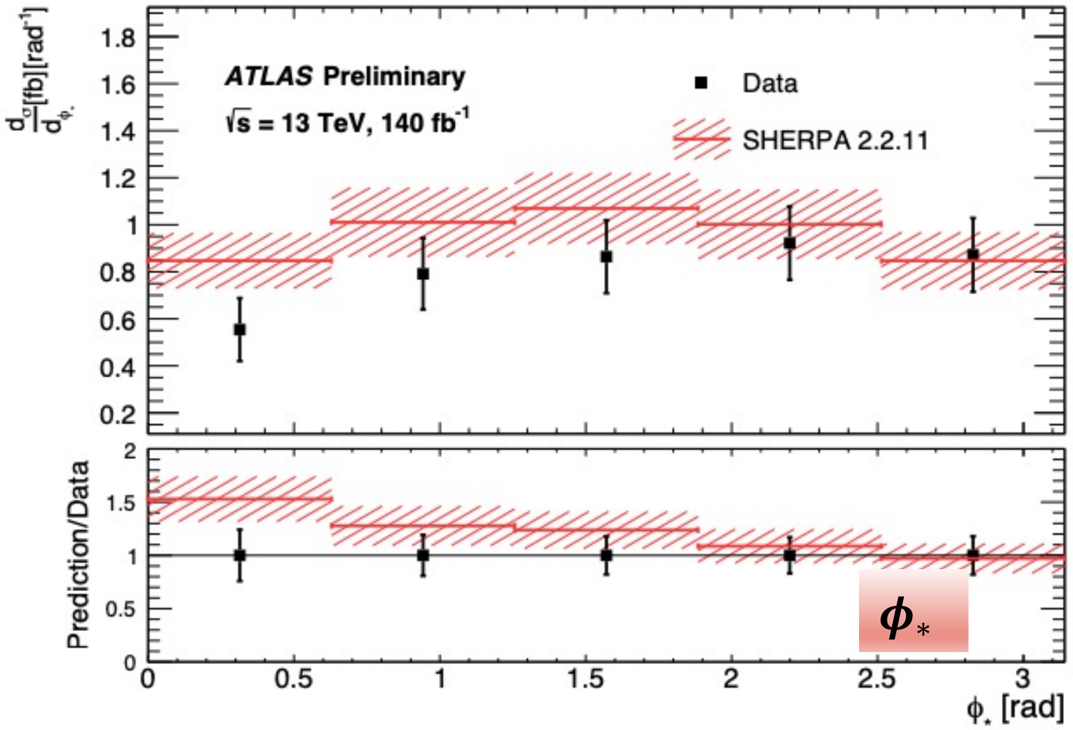

Search for neutral triple gauge couplings (nTGC) and measurement of Z(->ll)γ

- The precise measurement of the electroweak $Z\gamma$ production is a powerful test of the Standard Model (SM), particularly in the absence of hints of new physics beyond the SM.
- The neutral Triple Gauge Couplings (nTGCs) provide a unique pathway to the new physics beyond the SM as it can arise from SM effective field theory (SMEFT) operators that respect the full electroweak gauge group $SU(2)_L \otimes U(1)_Y$ of the SM at only the level of **dimension-8 or higher**.

$$\mathcal{L}_{\mathrm{SMEFT}} = \mathcal{L}_{\mathrm{SM}} + \sum_j \frac{\tilde{c}_j}{\tilde{\Lambda}^4} O_j = \mathcal{L}_{\mathrm{SM}} + \sum_j \frac{\mathrm{sign}(\tilde{c}_j)}{\Lambda_j^4} O_j = \mathcal{L}_{\mathrm{SM}} + \sum_j \frac{1}{[\Lambda_j^4]} O_j$$

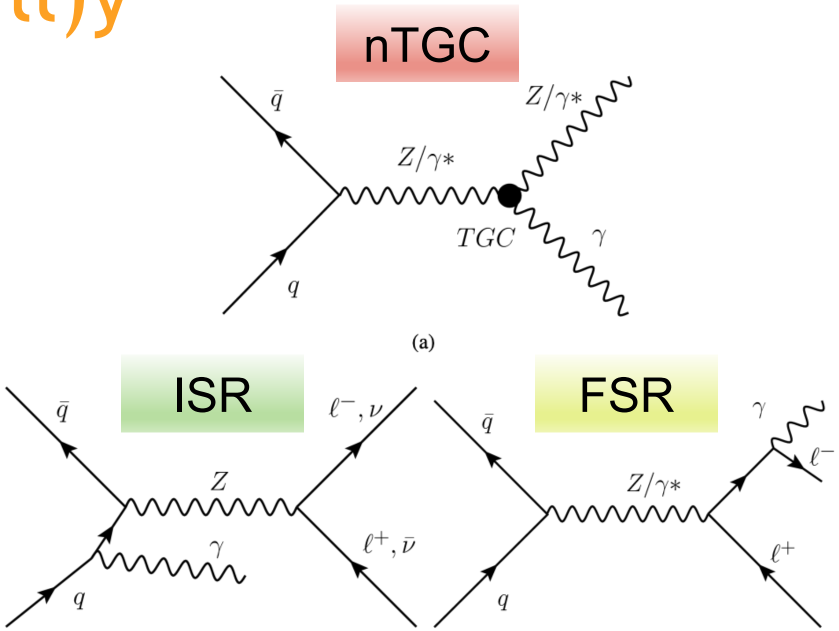

Requirements	Signal Region
Trigger	single or di-lepton triggers
N_{lepton}	≥ 2 OSSF leptons
Leading lepton p_T	> 30 GeV
N_{photon}	≥ 1 photon
Leading photon p_T	> 200 GeV
N_{jet}	exclusive, $= 0$
$m_{\ell\ell}$	$\lvert m_{\ell\ell} - m_Z\rvert < 10$ GeV
$m_{\ell\ell} + m_{\ell\ell\gamma}$	> 182 GeV

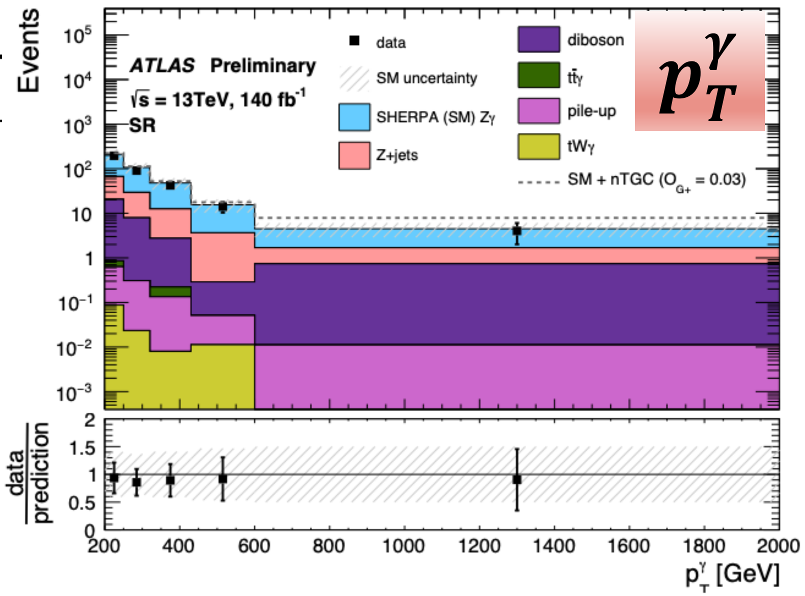

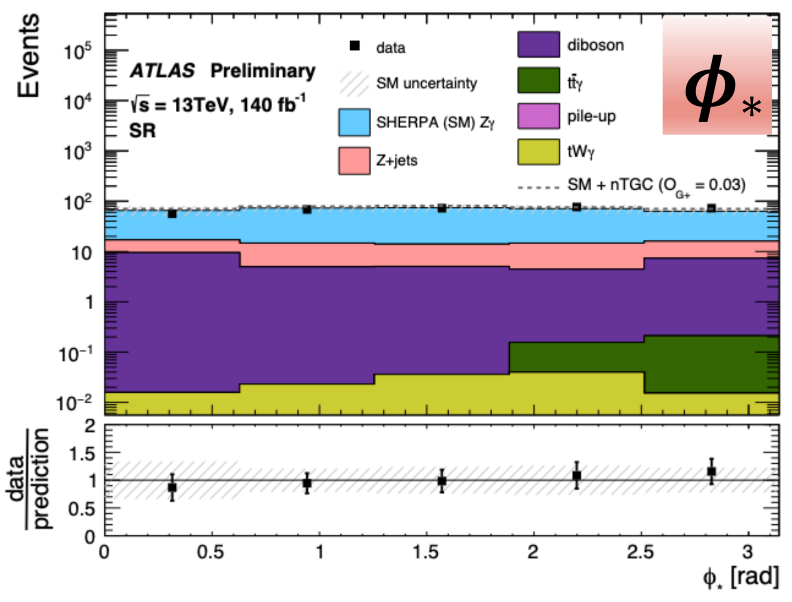

neutral Triple Gauge Couplings (nTGC) in $Z\gamma$ production

In the absence of deviations from the SM predictions, the measurement of the differential cross section as a function of p_T^{γ} is used to set limits on anomalous neutral triple gauge couplings.
The constraints on both Wilson coefficients in the SMEFT framework and ***form factors*** in the effective vertex approach are derived and they incorporate a ***fully gauge-invariant $SU(2)_L \otimes U(1)_Y$ symmetry***.

The 95% C.L. limits on two extra dimension-8 operators O_{G+} and O_{G-} parameterized with the fully gauge invariant nTGC formulation are presented for the first time at the LHC.
Under the updated formalism, the new limits on h_4^Z and h_4^{γ} differ by two orders of magnitude compared to previous ATLAS results.

A two-dimensional fit is also performed to obtain bounds for pairs of nTGC parameters. Constraints on each pair of nTGC parameters are shown in the form of ellipses at 95% C.L. on the (h_3^V, h_4^V) planes. It is also assumed that any excess in data over background predictions only comes from nTGC effects, and only two scanned parameters are varied while other parameters are set to zero at one time. The statistical constraints on h_4^{γ} and h_4^Z differ by a constant factor as defined in equation 4b. For completeness, we show the constraints on both parameters in the figure.

$$\mathcal{L}(c,\vec{\theta}) = \frac{1}{\sqrt{(2\pi)^k \cdot |\mathbf{V}|}} e^{-\frac{1}{2}\chi^2(c,\vec{\theta})} \prod_{\vec{\theta}} \mathcal{G}(\vec{\theta})$$

test statistic measures the agreement between the statistical model and the unfolded results

$$\chi^2(c,\vec{\theta}) = (\vec{y} - \vec{f}(c,\vec{\theta}))^T V^{-1} (\vec{y} - \vec{f}(c,\vec{\theta}))$$

Parameters	Limits at 95% C.L.	
	Observed 95% C.L.	Expected 95 % C.L.
h_4^{γ}	$[-1.3\times10^{-5}, 1.4\times10^{-5}]$	$[-1.5\times10^{-5}, 1.6\times10^{-5}]$
h_4^{Z}	$[-2.4\times10^{-5}, 2.6\times10^{-5}]$	$[-2.8\times10^{-5}, 3.0\times10^{-5}]$
h_3^{γ}	$[-3.5\times10^{-4}, 4.6\times10^{-4}]$	$[-4.0\times10^{-4}, 4.9\times10^{-4}]$
h_3^{Z}	$[-3.2\times10^{-4}, 3.2\times10^{-4}]$	$[-3.7\times10^{-4}, 3.6\times10^{-4}]$

$$h_4 = -\frac{1}{[\Lambda_{G+}^4]}\frac{v^2 M_Z^2}{s_W c_W}$$

$$h_4 = \frac{c_W}{s_W} h_4^{\gamma}$$

$$h_3^Z = \frac{1}{[\Lambda_{\widetilde{B}W}^4]}\frac{v^2 M_Z^2}{2 s_W c_W}$$

$$h_3^{\gamma} = -\frac{1}{[\Lambda_{G-}^4]}\frac{v^2 M_Z^2}{2 c_W^2}$$

Same-sign W boson polarisation

arXiv:2503.11317

- Study of diboson polarization probes gauge symmetry structure and electroweak symmetry breaking mechanism:
  - Longitudinal polarisation generated by Goldstone bosons in EWSB
  - Unitarity of $V_L\ V_L$ scattering cross-section at high energies guaranteed by gauge symmetry

- Measurement of production cross sections of polarised at with $W^{\pm}W^{\pm}$ at 13 TeV with 140 fb^{-1}
- Experiments gaining sensitivity to $V_L\ V_L$ production and starting to study energy dependence of cross-section

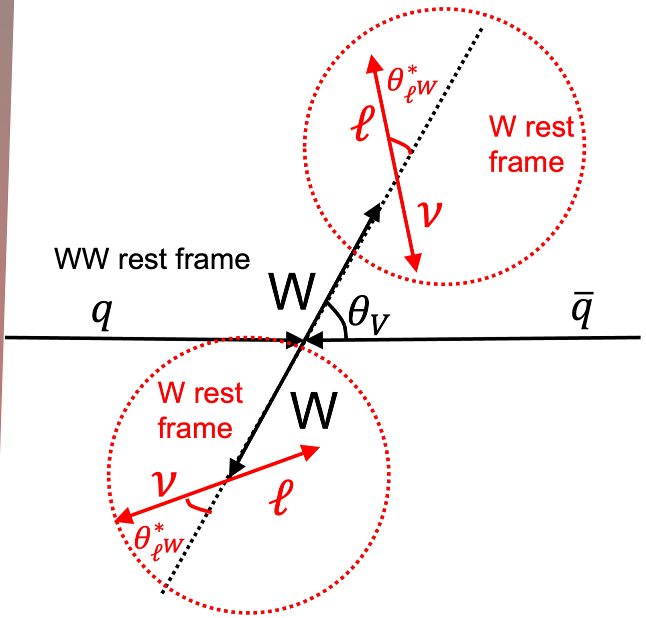

VBS EW $W^{\pm}W^{\pm}jj$ production

QCD $W^{\pm}W^{\pm}jj$ production

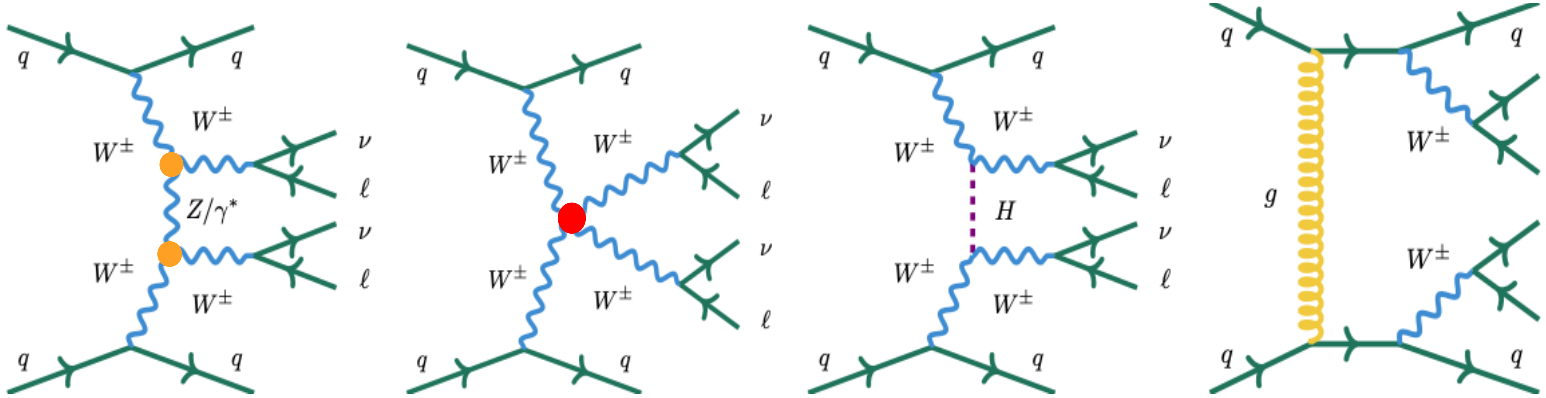

triple-gauge boson vertices

quartic gauge boson vertex

Higgs exchange

QCD $W^{\pm}W^{\pm}jj$ production

Same-sign W boson polarisation

- $\Delta\eta_{\ell\ell}, m_{\ell\ell}, \Delta\phi_{jj}, m_{jj}, m_T^{o}, m_T^{\ell_2}, p_T^{j_i}, \ldots$

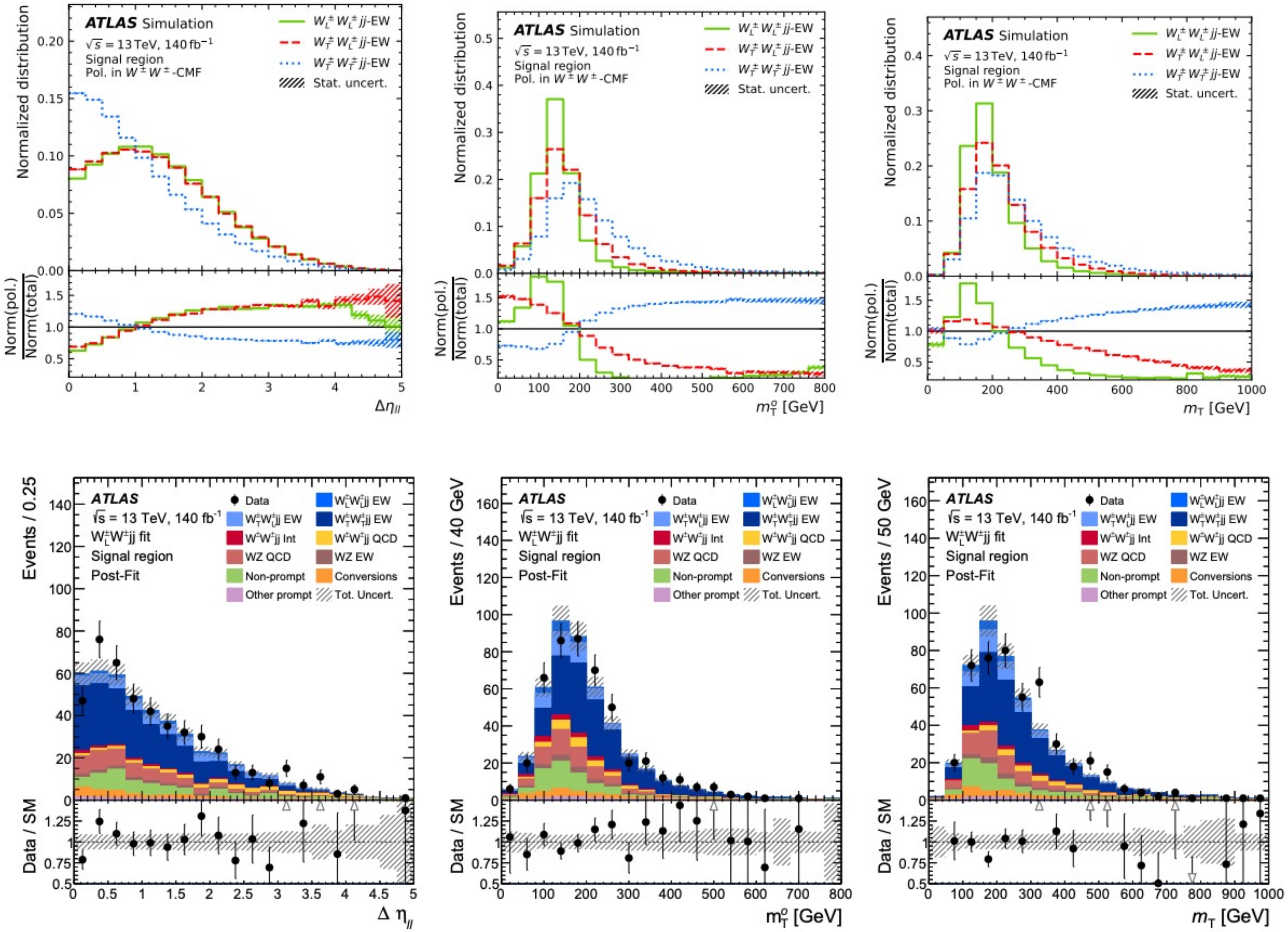

Same-sign W boson polarisation

- $\Delta\eta_{\ell\ell}, m_{\ell\ell}, \Delta\phi_{jj}, m_{jj}, m_T^{0}, m_T^{\ell_2}, p_T^{j_i}, \ldots$

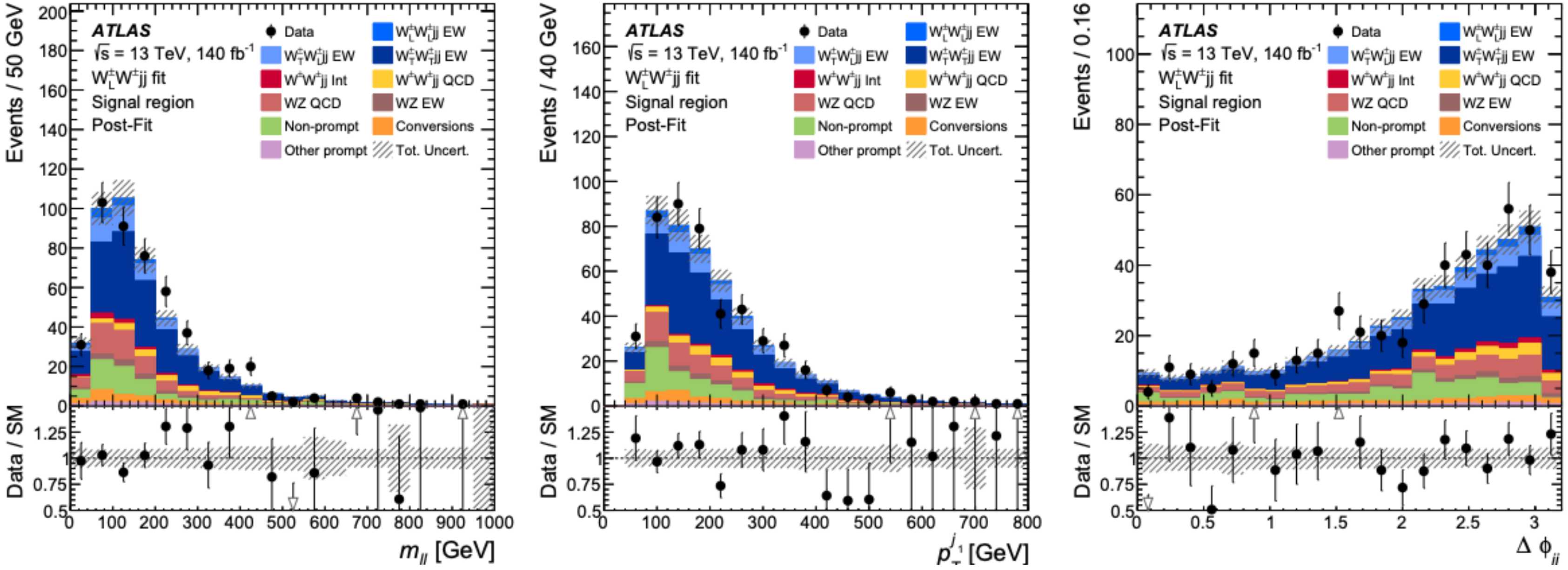

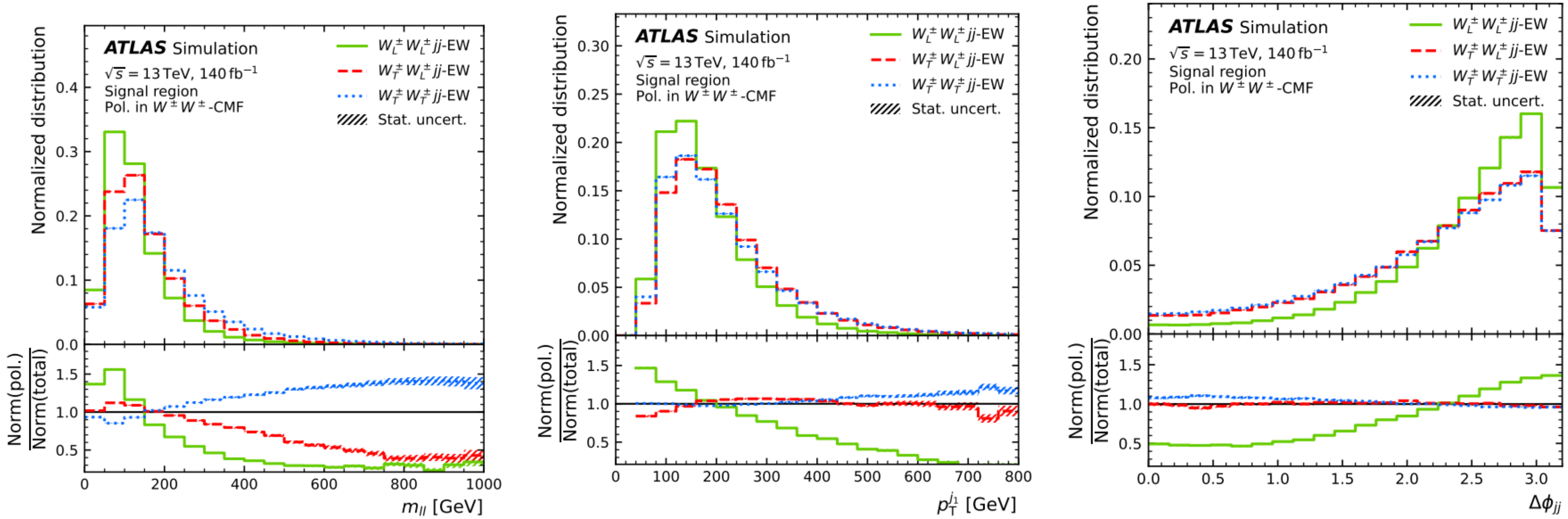

Same-sign W boson polarisation

- Two fits performed to extract the $W_L^\pm W_X^\pm$ and $W_T^\pm W_T^\pm$ ($W_L^\pm W_L^\pm$ and $W_T^\pm W_X^\pm$) polarisation fractions
  - Fit performed in 3 regions of $\mathrm{DNN}_{\mathrm{inclusive}}$, using $\text{LX-DNN}_{\text{signal}}$ as a polarisation discriminator
  - A low- m_{jj} and WZ CRs also enter the fit
- Evidence of $W_L^\pm W_X^\pm$ state: **3.3σ observed (4.0σ expected)**
- Measurement precision is **statistically** limited

	Region 1	Region 2	Region 3
Process	Region 0 to 0.3	Region 0.3 to 0.7	Region 0.7 to 1
$W_L^\pm W_L^\pm jj$	1.8 ± 0.7	5.6 ± 1.9	8.3 ± 2.8
$W_L^\pm W_T^\pm jj$	6.0 ± 2.5	17.8 ± 6.2	25.7 ± 8.5
$W_T^\pm W_T^\pm jj$	18.4 ± 4.4	64.0 ± 10.0	111.9 ± 14.7
QCD $W^\pm W^\pm jj$	14.4 ± 4.1	12.5 ± 3.5	2.6 ± 0.8
Int $W^\pm W^\pm jj$	2.3 ± 0.1	6.0 ± 0.2	4.8 ± 0.1
QCD $W^\pm Zjj$	33.3 ± 2.6	20.3 ± 1.6	4.5 ± 0.4
EW $W^\pm Zjj$	3.3 ± 0.1	6.2 ± 0.2	5.5 ± 0.2
Non-prompt	31.2 ± 4.3	20.2 ± 2.9	10.4 ± 3.1
Conversions	14.6 ± 3.7	6.2 ± 1.8	1.6 ± 0.5
Other prompt	3.7 ± 0.7	2.6 ± 0.6	0.8 ± 0.2
Total SM	129 ± 7	161 ± 10	176 ± 13
Data	142	158	175

Longitudinally polarized W bosons in the electroweak production of same-sign W boson pairs in association with two jets (arXiv:2503.11317)

$W^{\pm}W^{\pm} \longrightarrow \ell^{\pm}\nu\ell'^{\pm}\nu$ ➔ where ℓ and ℓ' can be e or μ

NEW March 2025!!!

Kinematics	Descriptions	Scaling
	Object-level variables	
$p_{\mathrm{T}}^{\ell_1}$	p_T of the leading lepton	$\log_{10}(x)$
$\eta^{\ell 1}$	η of the leading lepton	x
ℓ_1 type	Flavor of the leading lepton	x
$p_{\mathrm{T}}^{\ell_2}$	p_{T} of the subleading lepton	$\log_{10}(x)$
η^{ℓ_2}	η of the subleading lepton	x
$\phi^{\ell_2} - \phi^{\ell_1}$	Difference in azimuthal angle between the leading and subleading leptons	x
ℓ_2 type	Flavor of the subleading lepton	x
$p_{\mathrm{T}}^{j_1}$	p_{T} of the leading jet	$\log_{10}(x)$
η^{j_1}	η of the leading jet	x
$\phi^{j_1} - \phi^{\ell_1}$	Difference in azimuthal angle between the leading jet and leading lepton	x
$p_{\mathrm{T}}^{j_2}$	p_{T} of the subleading jet	$\log_{10}(x)$
η^{j_2}	η of the subleading jet	x
$\phi^{j_2} - \phi^{\ell_1}$	Difference in azimuthal angle between the subleading jet and leading lepton	x
$E_{\mathrm{T}}^{\mathrm{miss}}$	Missing transverse momentum	$\log_{10}(x)$
$\phi(E_{\mathrm{T}}^{\mathrm{miss}}) - \phi^{\ell_1}$	Difference in azimuthal angle between the missing transverse momentum and leading lepton	x
	Event-level variables	
$Z_{\ell_1}^{\star}$	Zeppenfeld variable of the leading lepton [64]	$\sqrt{x}$
$Z_{\ell_2}^{\star}$	Zeppenfeld variable of the subleading lepton [64]	$\sqrt{x}$
$m_{\mathrm{T}}^{\ell_1}$	Transverse mass of the leading lepton and $E_{\mathrm{T}}^{\mathrm{miss}}$	$\sqrt{x}$
$m_{\mathrm{T}}^{\ell_2}$	Transverse mass of the subleading lepton and $E_{\mathrm{T}}^{\mathrm{miss}}$	$\sqrt{x}$
$\Delta R_{\ell\ell}$	Distance ΔR between the leading and subleading leptons	x
$\Delta\eta_{\ell\ell}$	Difference in pseudorapidity between the leading and subleading leptons	$\sqrt{x}$
$m_{\ell\ell}$	Invariant mass of the two leptons	$\log_{10}(x)$
$p_{\mathrm{T}}^{\ell\ell}$	p_{T} of the dilepton system	$\sqrt{x}$
m_{T}	Transverse mass of the dilepton system and $E_{\mathrm{T}}^{\mathrm{miss}}$ [20]	$\sqrt{x}$
m_{T}^{o}	Projected transverse mass $\sqrt{(p_{\mathrm{T}}^{\ell_1} + p_{\mathrm{T}}^{\ell_2} + E_{\mathrm{T}}^{\mathrm{miss}})^2 - (\vec{p_{\mathrm{T}}}^{\ell_1} + \vec{p_{\mathrm{T}}}^{\ell_2} + \vec{E}_{\mathrm{T}}^{\mathrm{miss}})^2}$ [65]	$\sqrt{x}$
ΔR_{jj}	Distance ΔR between the leading and subleading jets	x
Δy_{jj}	Rapidiy difference between the leading and subleading jets	x
m_{jj}	Invariant mass of the two jets	$\log_{10}(x)$
$\Delta\phi_{jj}$	Difference in azimuthal angle between the leading and subleading jets	x
$(p_{\mathrm{T}}^{\ell_1} \cdot p_{\mathrm{T}}^{\ell_2})/(p_{\mathrm{T}}^{j_1} \cdot p_{\mathrm{T}}^{j_2})$	p_{T} ratio of the leptons and jets [22]	$\log_{10}(x + 0.02)$
$\min(\Delta R_{\ell,j})$	Minimal distance ΔR between the leptons and jets	x

Variables used in the training and optimization of the DNNs. The variables are scaled with different scaling functions for the training and application.

VBS: same-sign W boson scattering in events with one tau lepton

Submitted to J. High Energy Phys. - [arXiv:2410.04210]

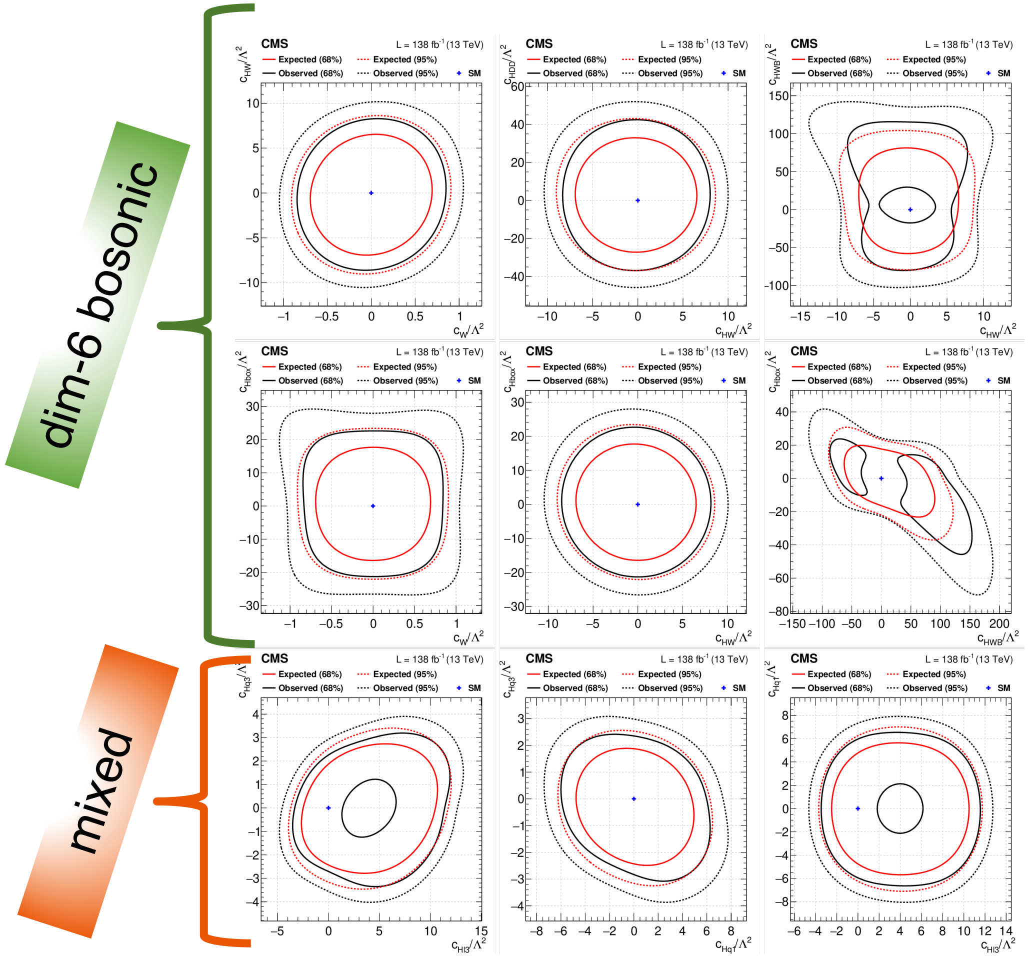

Observed (black) and expected (red) 68 (solid) and 95% (dashed) CL contours for –2 ln ΔL as functions of the reported dim-6 bosonic (upper two rows) and mixed (lower row) Wilson coefficient pairs. When there are two contours for the same CL value, the constrained set of Wilson coefficient values is represented by the area between the two of them if they are concentric, otherwise it consists of the internal areas of the contours.

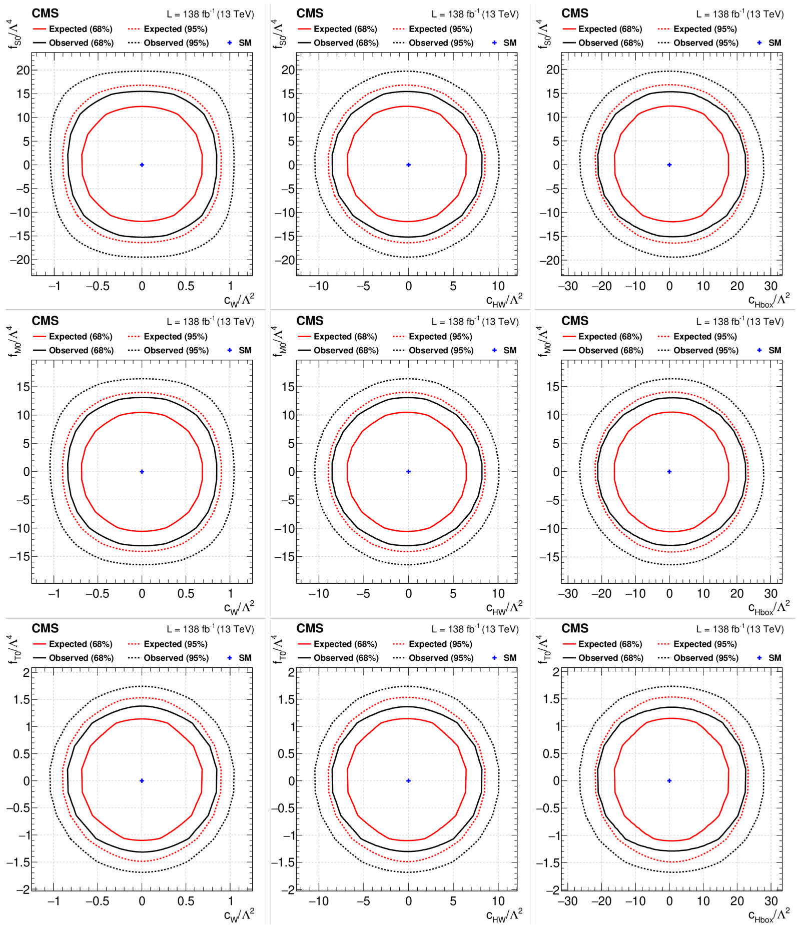

Observed (black) and expected (red) 68 (solid) and 95% (dashed) CL contours for –2 ln ΔL as functions of the reported (dim-6, dim-8)Wilson coefficient pairs.

VBS Fully- and semi-leptonic final states combination

CMS-PAS-SMP-24-013

$W^{\pm}W^{\pm}$, $W^{\pm}W^{\mp}$, $W^{\pm}Z$, ZZ Combination

All selected events feature:

- ≥ 2 jets with a high invariant mass and large pseudorapidity separation

$$m_{jj}^{VBS} > 500, 300 \; or \; 100 GeV$$
$$\left|\Delta\eta_{jj}^{VBS}\right| > 2.5$$

- ≥ 1 heavy vector boson decaying leptonically

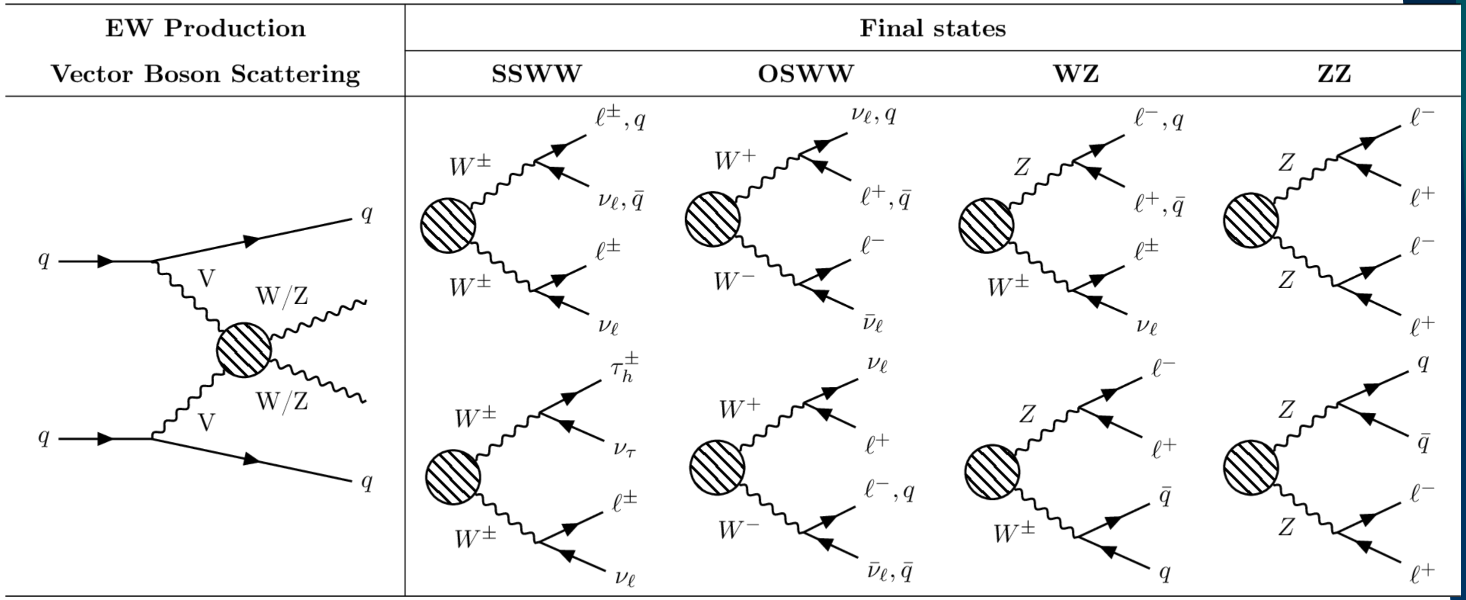

Test Statistic: Profile likelihood ratio q
parameter of interest: signal strength μ

$$q(\vec{\mu}) = -2\log \frac{L(\vec{x}|\vec{\mu}, \hat{\hat{\vec{\theta}}})}{L(\vec{x}|\hat{\vec{\mu}}, \hat{\vec{\theta}})}$$

$$L(\vec{x}|\vec{\mu},\vec{\theta}) = \prod_{\text{bin}=k} \frac{(\vec{\mu}\cdot\vec{s}_k + b_k)^{n_k}}{n_k!} e^{-(\vec{\mu}\cdot\vec{s}_k + b_k)} \cdot \prod_{\text{syst}=j} \pi(\tilde{\theta}_j|\theta_j)$$

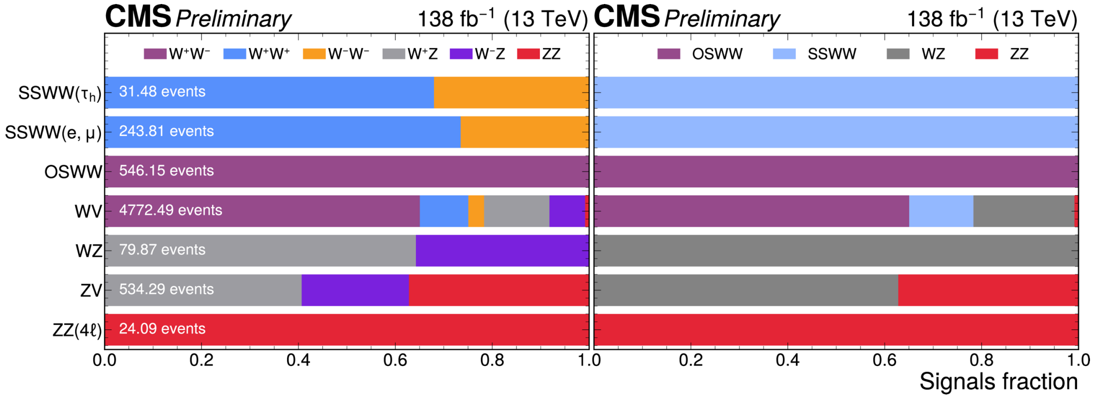

VBS Fully- and semi-leptonic final states combination

CMS-PAS-SMP-24-013

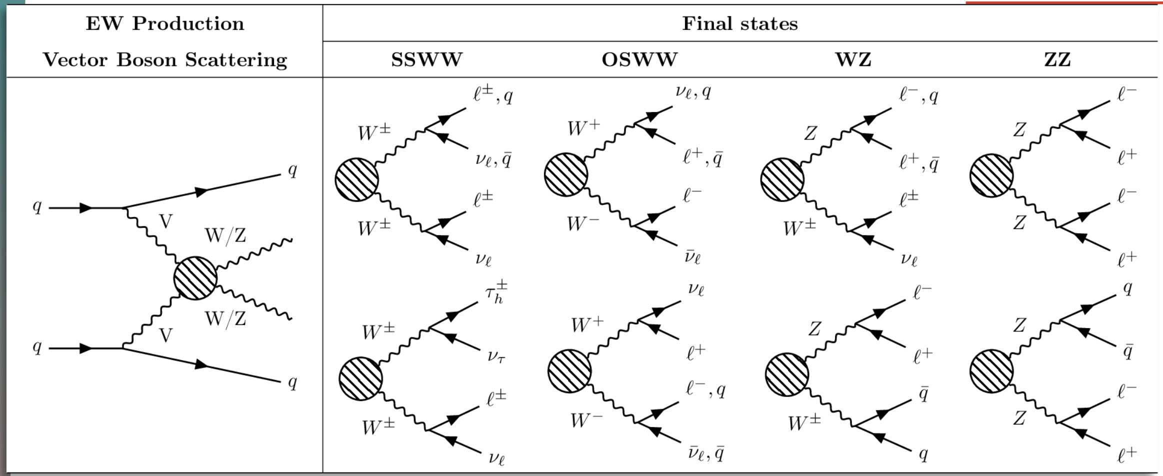

$W^{\pm}W^{\pm}$, $W^{\pm}W^{\mp}$, $W^{\pm}Z$, ZZ Combination

All selected events feature:

- ≥ 2 jets with a high invariant mass and large pseudorapidity separation
- ≥ 1 heavy vector boson decaying leptonically
- Mixed approach using machine learning (DNN, BDT) and traditional variables to separate signal and backgrounds depending on the channel

Two combination models:

- Test Statistic: Profile likelihood ratio
- **4-POIs:** four parameters of interest - signal strengths μ_{OSWW}, μ_{SSWW}, μ_{WZ}, μ_{ZZ}
- **6-POIs:** six parameters of interest - signal strengths $\mu_{W^+W^+}$, $\mu_{W^-W^-}$, $\mu_{W^+W^-}$, μ_{W^+Z}, μ_{W^-Z}, μ_{ZZ}

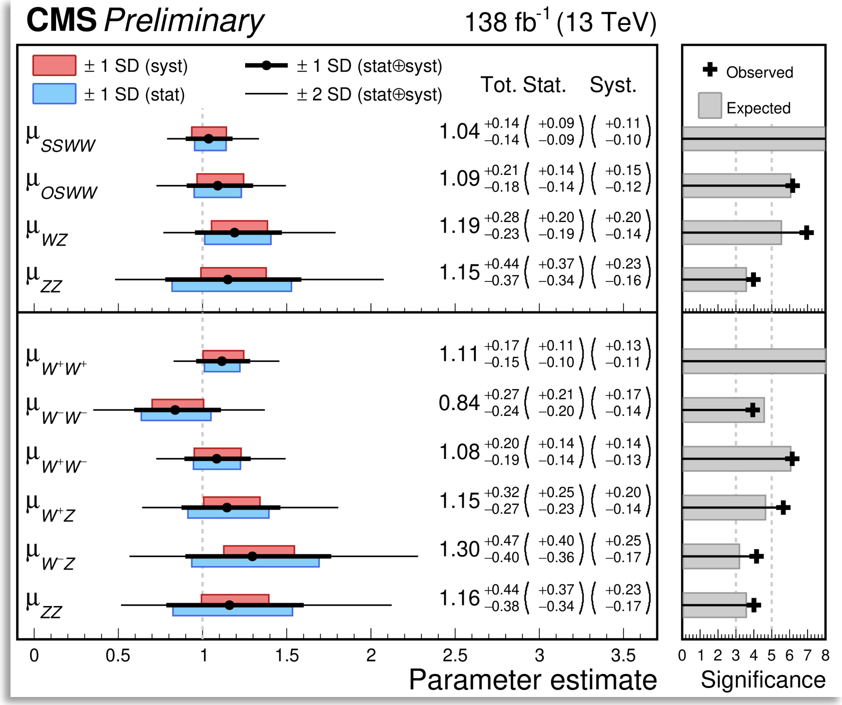

		OSWW	SSWW		WZ		ZZ
4-POI	μ	$1.09^{+0.21}_{-0.18}$ $\left(^{+0.20}_{-0.19}\right)$	$1.04^{+0.14}_{-0.14}$ $\left(^{+0.14}_{-0.14}\right)$		$1.19^{+0.28}_{-0.23}$ $\left(^{+0.29}_{-0.24}\right)$		$1.15^{+0.44}_{-0.37}$ $\left(^{+0.44}_{-0.37}\right)$
	σ	6.2 (6.1)	≫ 5 (≫ 5)		7.0 (5.5)		4.0 (3.6)
		W^+W^-	W^+W^+	W^-W^-	W^+Z	W^-Z	ZZ
6-POI	μ	$1.08^{+0.20}_{-0.19}$ $\left(^{+0.18}_{-0.18}\right)$	$1.11^{+0.17}_{-0.15}$ $\left(^{+0.14}_{-0.16}\right)$	$0.84^{+0.27}_{-0.24}$ $\left(^{+0.28}_{-0.25}\right)$	$1.15^{+0.32}_{-0.27}$ $\left(^{+0.32}_{-0.27}\right)$	$1.30^{+0.47}_{-0.40}$ $\left(^{+0.44}_{-0.37}\right)$	$1.16^{+0.44}_{-0.38}$ $\left(^{+0.42}_{-0.35}\right)$
	σ	6.1 (6.1)	≫ 5 (≫ 5)	4.0 (4.6)	5.7 (4.7)	4.2 (3.2)	4.0 (3.6)

Signal strengths are in agreement with the SM predictions within the 68% CL

VBS Fully- and semi-leptonic final states combination

$W^\pm W^\pm$, $W^\pm W^\mp$, $W^\pm Z$, ZZ Combination

CMS-PAS-SMP-24-013

Two combination models:

- **4-POIs:** four parameters of interest - signal strengths μ_{OSWW}, μ_{SSWW}, μ_{WZ}, μ_{ZZ}
- **6-POIs:** six parameters of interest - signal strengths $\mu_{W^+W^+}$, $\mu_{W^-W^-}$, $\mu_{W^+W^-}$, μ_{W^+Z}, μ_{W^-Z}, μ_{ZZ}

4-POIs	OSWW	SSWW	WZ	ZZ
Observed σ (Expected σ)	6.2 (6.1)	$\gg 5$ ($\gg 5$)	7.0 (5.5)	4.0 (3.6)

6-POIs	W^+W^-	W^+W^+	W^-W^-	W^+Z	W^-Z	ZZ
Observed σ (Expected σ)	6.1 (6.1)	$\gg 5$ ($\gg 5$)	4.0 (4.6)	5.7 (4.7)	4.2 (3.2)	4.0 (3.6)

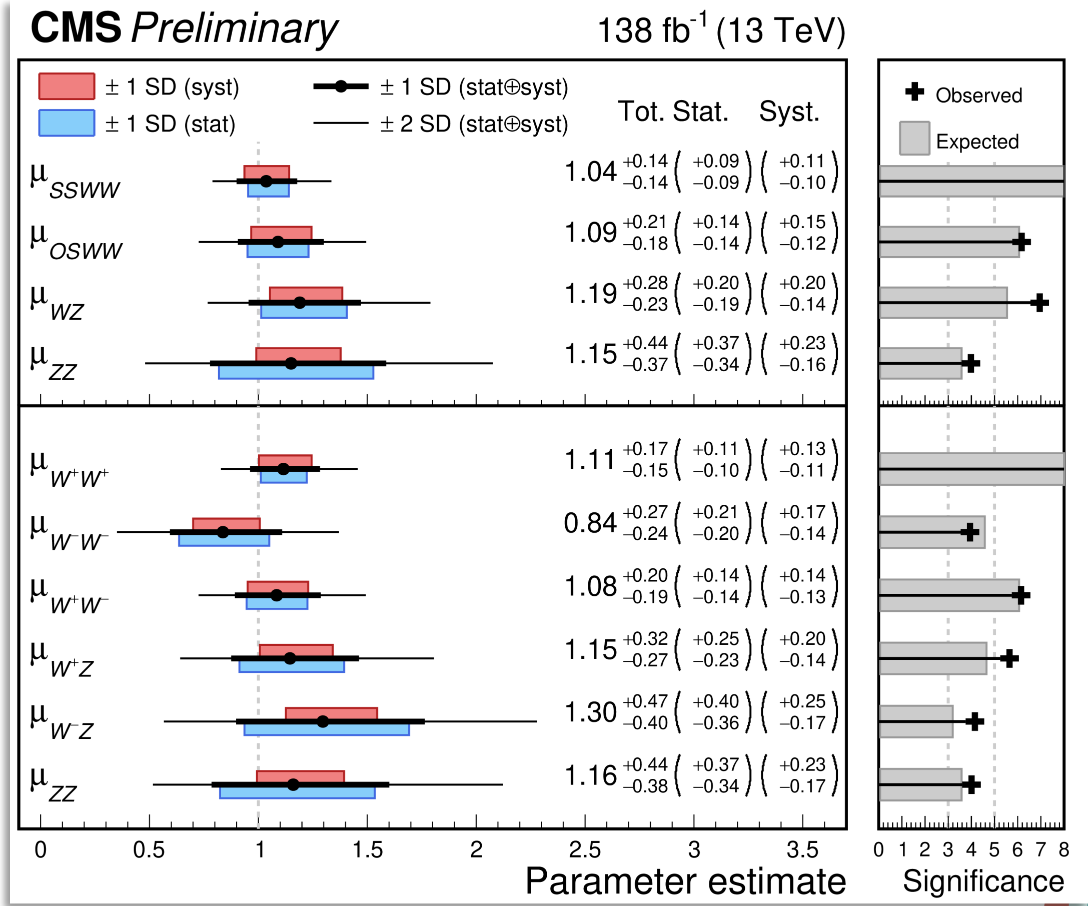

Signal strengths are in agreement with the SM predictions within the 68% CL

VBS Fully- and semi-leptonic final states combination

CMS-PAS-SMP-24-013

Region	n. ℓ	n. τ_h	SF	$\lvert\sum$ ch.$\rvert$	b-veto	$m_{\ell\ell}$	m_{jj}^{VBS}	$\lvert\Delta\eta_{jj}^{\mathrm{VBS}}\rvert$	n. AK4	n. AK8	m_V
WV-SR(Res)	1	0	-	1	✓	-	> 500	> 2.5	≥ 4	0	$\in [65, 105]$
WV-SR(Boost)	1	0	-	1	✓	-	> 500	> 2.5	≥ 2	1	$\in [70, 115]$
WV-Top(Res)	1	0	-	1	✗	-	> 500	> 2.5	≥ 4	0	$\in [65, 105]$
WV-Top(Boost)	1	0	-	1	✗	-	> 500	> 2.5	≥ 2	1	$\in [70, 115]$
WV-Wjets(Res)	1	0	-	1	✓	-	> 500	> 2.5	≥ 4	0	$\notin [65, 105]$
WV-Wjets(Boost)	1	0	-	1	✓	-	> 500	> 2.5	≥ 2	1	$\notin [70, 115]$
SSWW(τ_h)-SR	1	1	-	2	✓	-	> 500	> 2.5	≥ 2	-	-
SSWW(τ_h)-Top	1	1	-	0	✗	-	> 500	> 2.5	≥ 2	-	-
SSWW(τ_h)-OS	1	1	-	0	✓	-	> 500	> 2.5	≥ 2	-	-
SSWW(e,μ)-SR	2	0	-	2	✓	> 20	> 500	> 2.5	≥ 2	-	-
SSWW(e,μ)-b	2	0	-	2	✗	> 20	> 500	> 2.5	≥ 2	-	-
OS-SR(SF)	2	0	✓	0	✓	> 120	> 300	> 2.5	≥ 2	-	-
OS-SR(DF)	2	0	✗	0	✓	> 50	> 300	> 2.5	≥ 2	-	-
ZV-SR-b(Res)	2	0	✓	0	✗	$\in [76, 106]$	> 500	> 2.5	≥ 4	0	$\in [65, 105]$
ZV-SR-b(Boost)	2	0	✓	0	✗	$\in [76, 106]$	> 500	> 2.5	≥ 2	1	$\in [65, 105]$
ZV-SR(Res)	2	0	✓	0	✓	$\in [76, 106]$	> 500	> 2.5	≥ 4	0	$\in [65, 105]$
ZV-SR(Boost)	2	0	✓	0	✓	$\in [76, 106]$	> 500	> 2.5	≥ 2	1	$\in [65, 105]$
ZV-DY-b(Res)	2	0	✓	0	✗	$\in [76, 106]$	> 500	> 2.5	≥ 4	0	$\notin [65, 105]$
ZV-DY-b(Boost)	2	0	✓	0	✗	$\in [76, 106]$	> 500	> 2.5	≥ 2	1	$\notin [65, 105]$
ZV-DY(Res)	2	0	✓	0	✓	$\in [76, 106]$	> 500	> 2.5	≥ 4	0	$\notin [65, 105]$
ZV-DY(Boost)	2	0	✓	0	✓	$\in [76, 106]$	> 500	> 2.5	≥ 1	1	$\notin [65, 105]$
OSWW-DY(DF)	2	0	✗	0	✓	$\in [50, 80]$	> 300	> 2.5	≥ 2	-	-
OSWW-DY(SF)	2	0	✓	0	✓	$\in [76, 106]$	> 300	> 2.5	≥ 2	-	-
OSWW-Top(SF)	2	0	✓	0	✗	> 120	> 300	> 2.5	≥ 2	-	-
OSWW-Top(DF)	2	0	✗	0	✗	> 50	> 300	> 2.5	≥ 2	-	-
WZ-SR	3	0	✓(Z)	1	✓	$\in [76, 106]$	> 500	> 2.5	≥ 2	-	-
WZ-b	3	0	✓(Z)	1	✗	$\in [76, 106]$	> 500	> 2.5	≥ 2	-	-
ZZ(4ℓ)-SR	4	0	✓(Z)	0	-	$\in [60, 120]$	> 100	> 2.5	≥ 2	-	-

Analysis	Region	Subregions	Observable	Bins
WV	SR Resolved	(e, μ)	DNN resolved	25
WV	SR Boosted	(e, μ)	DNN boosted	12
WV	CR Top Resolved	(e, μ)	Events	1
WV	CR Top Boosted	(e, μ)	Events	1
WV	CR W+jets Resolved	(e, μ)	$p_T^{W\to\ell\nu}$	21
WV	CR W+jets Boosted	(e, μ)	$p_T^{W\to\ell\nu} : p_{T,j_2}^{\mathrm{VBS}}$	7
ZV	SR Resolved b-tag	-	DNN resolved b-tag	21
ZV	SR Boosted b-tag	-	DNN boosted b-tag	21
ZV	SR Resolved b-veto	-	DNN resolved b-veto	21
ZV	SR Boosted b-veto	-	DNN boosted b-veto	21
ZV	CR DY Resolved	b-tag, b-veto (2017,2018)	$p_T^{Z\to\ell\ell} : p_{T,j_2}^{\mathrm{VBS}}$	12
ZV	CR DY Resolved	b-tag, b-veto (2016)	$p_T^{Z\to\ell\ell}$	5
ZV	CR DY Boosted	b-tag, b-veto	$p_T^{Z\to\ell\ell}$	5
OSWW	SR	$e\mu$ ($Z_{\ell\ell} \lesseqgtr 1$)	DNN	13
OSWW	SR	ee, $\mu\mu$ ($Z_{\ell\ell} \lesseqgtr 1$)	$m_{jj}^{\mathrm{VBS}} : \Delta\eta_{jj}^{\mathrm{VBS}}$	8
OSWW	CR Top	($ee, \mu\mu, e\mu$)	Events	1
OSWW	CR DY	($e\mu$)	Events	1
OSWW	CR DY	(ee, $\mu\mu$, $\lvert\Delta\eta_{jj}^{\mathrm{VBS}}\rvert \lesseqgtr 5$)	Events	1
SSWW(e,μ)	SR	-	$m_{jj}^{\mathrm{VBS}} : m_{ll}$	32
SSWW(e,μ)	CR b-tag	-	m_{jj}^{VBS}	4
WZ	SR	-	BDT	8
WZ	CR b-tag	-	m_{jj}^{VBS}	4
ZZ(4ℓ)	SR	($4e, 4\mu, 2e2\mu$)	K_D discriminant	25
SSWW(τ_h)	SR	(e, μ)	DNN	12
SSWW(τ_h)	CR Top	(e, μ)	DNN	12
SSWW(τ_h)	CR OS	(e, μ)	DNN	12

neutral Triple Gauge Couplings (nTGC) in Zγ production

Newly generalized form factor formulation for neutral triple gauge vertices

- ($h_3^Z, h_3^\gamma, h_4^\gamma$) map to the effective cutoff scale $\Lambda_i^4 \equiv \frac{\mathcal{O}_i}{\Lambda_i^4}$ where i= G⁺, G⁻ , B̃W
- Constraints on Wilson coefficients and ***form factors*** ➔ first attempt to incorporate a ***fully gauge-invariant $SU(2)_L \otimes U(1)_Y$ symmetry***
- Superseding former $U(1)_{em}$ only formulation
- New limits on h_4^Z and h_4^γ differ by two orders of magnitude compared to previous ATLAS results due to the updated formulation
- 2D parametrization: interference between two Wilson coefficients taken into account

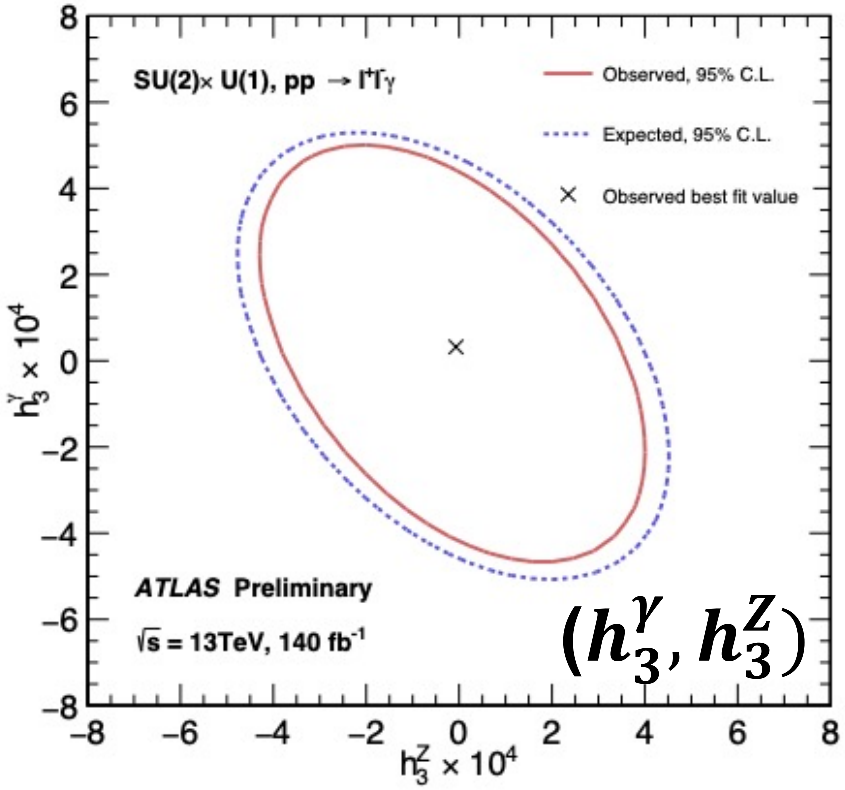

form factors

Parameters	Limits at 95% C.L.	
	Observed 95% C.L.	Expected 95 % C.L.
h_4^γ	$[-1.3\times10^{-5}, 1.4\times10^{-5}]$	$[-1.5\times10^{-5}, 1.6\times10^{-5}]$
h_4^Z	$[-2.4\times10^{-5}, 2.6\times10^{-5}]$	$[-2.8\times10^{-5}, 3.0\times10^{-5}]$
h_3^γ	$[-3.5\times10^{-4}, 4.6\times10^{-4}]$	$[-4.0\times10^{-4}, 4.9\times10^{-4}]$
h_3^Z	$[-3.2\times10^{-4}, 3.2\times10^{-4}]$	$[-3.7\times10^{-4}, 3.6\times10^{-4}]$

$$h_3^Z = \frac{1}{[\Lambda_{\tilde{B}W}^4]}\frac{v^2M_Z^2}{2s_Wc_W} \qquad h_4 = -\frac{1}{[\Lambda_{G+}^4]}\frac{v^2M_Z^2}{s_Wc_W}$$

$$h_3^\gamma = -\frac{1}{[\Lambda_{G-}^4]}\frac{v^2M_Z^2}{2c_W^2} \qquad h_4 = \frac{c_W}{s_W}h_4^\gamma$$

- $s_W = sin\theta_W$
- $c_W = cos\theta_W$
- v = *Higgs field vacuum expectation value*

neutral Triple Gauge Couplings (nTGC) in $Z\gamma$ production

Newly generalized form factor formulation for neutral triple gauge vertices

- $(h_3^Z, h_3^\gamma, h_4^\gamma)$ map to the effective cutoff scale $\Lambda_i^4 \equiv \frac{\mathcal{O}_i}{\Lambda_i^4}$ where i= G⁺, G⁻ , B̃W
- Constraints on Wilson coefficients and ***form factors*** ➔ first attempt to incorporate a ***fully gauge-invariant $SU(2)_L \otimes U(1)_Y$ symmetry***
- Superseding former $U(1)_{em}$ only formulation
- New limits on h_4^Z and h_4^γ differ by two orders of magnitude compared to previous ATLAS results due to the updated formulation
- 2D parametrization: interference between two Wilson coefficients taken into account

Wilson coefficients in the SMEFT framework

Parameters	Limits at 95% C.L.	
	Observed 95% C.L.	Expected 95 % C.L.
O_{G+}	[-0.022, 0.020]	[-0.025, 0.023]
O_{G-}	[-1.41, 1.08]	[-1.50, 1.23]
O_{BB}	[-0.37, 0.37]	[-0.44, 0.44]
$O_{\tilde{B}W}$	[-0.54, 0.53]	[-0.62, 0.61]
O_{BW}	[-0.87, 0.95]	[-1.05, 1.14]
O_{WW}	[-1.90, 1.78]	[-2.26, 2.13]

The 95% C.L. limits on two extra dimension-8 operators O_{G+} and O_{G-} parameterized with the fully gauge invariant nTGC formulation are presented for the first time at the LHC

$Z\gamma(\ell\ell\gamma)$ Production: Constraints on Energy Scale Λ_i